AD-A098 407 FOREIGN TECHNOLOGY DIV WRIGHT-PATTERSON AFB OH F/G 20/7
HIGH-CURRENT BETATRON AND STEREOBETATRON,(U)
FEB 81 A A BOROBYEV, V A MOSKALEV
UNCLASSIFIED FTD-ID(RS)T-1715-80 NL

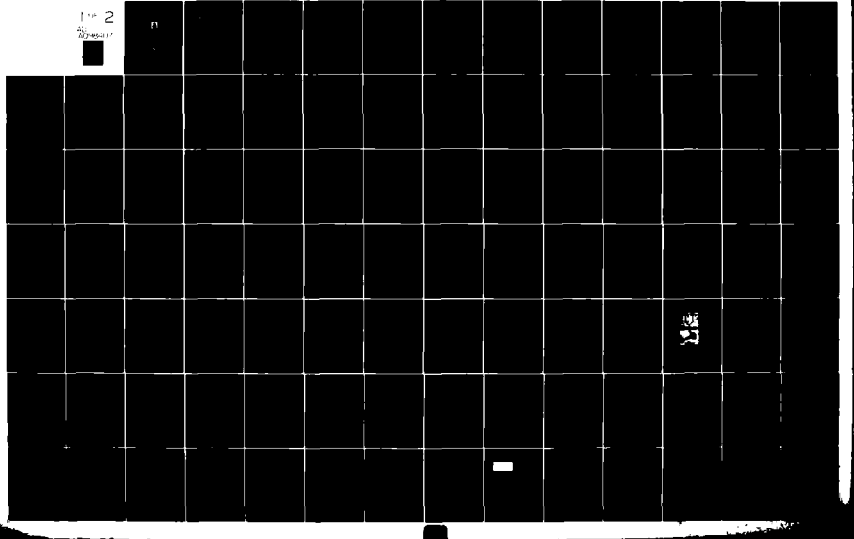

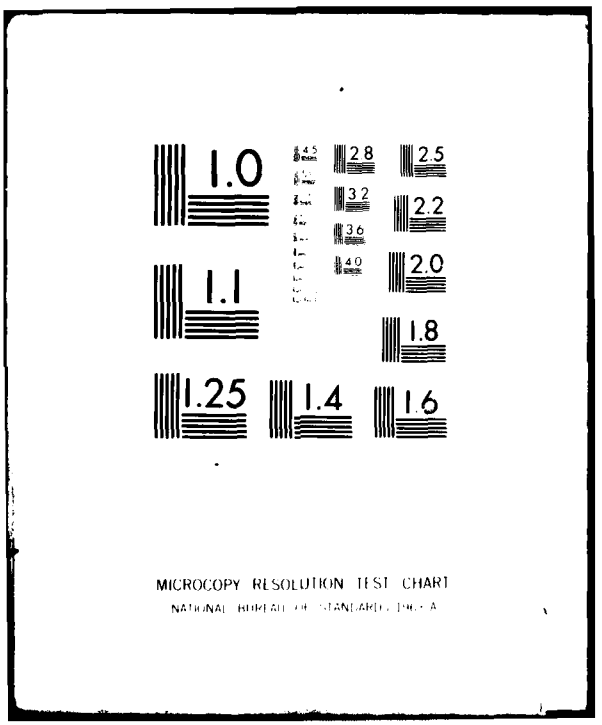
1.0
1.1
1.25
1.4
1.6
1.8
2.0
2.2
2.5
2.8
3.2
3.6
4.0
MICROCOPY RESOLUTION TEST CHART
NATIONAL BUREAU OF STANDARDS 1963-A

(2)

FTD-ID(RS)T-1715-80

AD A098407

FOREIGN TECHNOLOGY DIVISION

HIGH-CURRENT BETATRON AND STEREOBETATRON

by

A. A. Borobyev, V. A. Moskalev

Approved for public release;
distribution unlimited.

UNEDITED MACHINE TRANSLATION

FTD-ID(RS)T-1715-80 4 February 1981

MICROFICHE NR: FTD-81-C-000017

HIGH-CURRENT BETATRON AND STEREOBETATRON

By: A. A./Borobyev, V. A./Moskalev

English pages: 161

Source: Sil'notochnyy Betatron i Stereobetatron, Atomizdat, Moscow, 1969, pp. 1-103.

Country of origin: USSR
This document is a machine translation
Requester: FTD/TQTD
Approved for public release; distribution unlimited.

PREPARED BY:

TRANSLATION DIVISION
FOREIGN TECHNOLOGY DIVISION
WP-AFB, OHIO.

TABLE OF CONTENTS

U. S. Board on Geographic Names Transliteration System..... ii

Preface..... 3

Introduction..... 5

Chapter 1. Theoretical Fundamentals of Obtaining High Currents in the Betatron. Magnetic Field and Electromagnet... 12

Chapter 2. High-Voltage Injection of Electrons Into a Chamber of a High-Current Betatron..... 37

Chapter 3. System of Shift of Accelerated Electrons From Equilibrium Orbit to Target..... 66

Chapter 4. Some Characteristics of Beam and Results of the Laboratory Tests of High-Current Betatron..... 88

Chapter 5. Two-Chamber Sterobetatron..... 126

References..... 161

U. S. BOARD ON GEOGRAPHIC NAMES TRANSLITERATION SYSTEM

Block	Italic	Transliteration	Block	Italic	Transliteration
А а	*А а*	A, a	Р р	*Р р*	R, r
Б б	*Б б*	B, b	С с	*С с*	S, s
В в	*В в*	V, v	Т т	*Т т*	T, t
Г г	*Г г*	G, g	У у	*У у*	U, u
Д д	*Д д*	D, d	Ф ф	*Ф ф*	F, f
Е е	*Е е*	Ye, ye; E, e*	Х х	*Х х*	Kh, kh
Ж ж	*Ж ж*	Zh, zh	Ц ц	*Ц ц*	Ts, ts
З з	*З з*	Z, z	Ч ч	*Ч ч*	Ch, ch
И и	*И и*	I, i	Ш ш	*Ш ш*	Sh, sh
Й й	*Й й*	Y, y	Щ щ	*Щ щ*	Shch, shch
К к	*К к*	K, k	Ъ ъ	*Ъ ъ*	"
Л л	*Л л*	L, l	Ы ы	*Ы ы*	Y, y
М м	*М м*	M, m	Ь ь	*Ь ь*	'
Н н	*Н н*	N, n	Э э	*Э э*	E, e
О о	*О о*	O, o	Ю ю	*Ю ю*	Yu, yu
П п	*П п*	P, p	Я я	*Я я*	Ya, ya

*ye initially, after vowels, and after ъ, ь; e elsewhere.
When written as ë in Russian, transliterate as yë or ë.

RUSSIAN AND ENGLISH TRIGONOMETRIC FUNCTIONS

Russian	English	Russian	English	Russian	English
sin	sin	sh	sinh	arc sh	sinh^{-1}
cos	cos	ch	cosh	arc ch	cosh^{-1}
tg	tan	th	tanh	arc th	tanh^{-1}
ctg	cot	cth	coth	arc cth	coth^{-1}
sec	sec	sch	sech	arc sch	sech^{-1}
cosec	csc	csch	csch	arc csch	csch^{-1}

Russian	English
rot	curl
lg	log

HIGH-CURRENT BETATRON AND STEREOBETATRON.

A. A. Vorobyev, V. A. Moskalev.

Page 2. A. A. Vorobyev, V. A. Moskalev.

High-current betatron and stereobetatron. M., Atomizdat, 1969.

The book contains the original material, dedicated to the developments of new induction accelerators - high-current betatrons and stereobetatrons. Are examined the fundamental questions, which appear during the planning, installation and the operation of the high-current betatrons: calculation and obtaining of the required magnetic field of accelerators, high-voltage system of the injection of electrons in the acceleration, system of the beam displacement of the accelerated electrons from the equilibrium orbit to the target, etc.

At the end of the book are given the materials on the correction of magnetic field in the two-chamber stereobetatrons, developed in Tomsk Polytechnic Institute, and also some original methods of obtaining the uniform in the azimuth controlling magnetic field, which does not require the subsequent correction.

The book is intended for scientific workers, graduate students and engineers, who are interested in an increase in the effectiveness in the work of the induction electron accelerators.

In the book 21 figures, 4 tables. At the end is given the bibliography of 15 designations.

PREFACE.

The problem of an increase in the accelerated current and intensity of the radiation/emission of charged particle accelerators is at present most urgent/actual and interests any developer of accelerator facilities.

In Tomsk polytechnic institute during the latter/last several years were carried out the scientific investigations and the technical-enginsering developments, directed toward a sharp increase in the current of the electrons, accelerated in the induction accelerators - betatrons. The result of these developments was the creation of the original electron accelerators of the high-current betatrons in which circulating in orbit electronic current reaches hundreds of amperes, and a number of accelerated in the cycle electrons is approximately $3 \cdot 10^{12}$.

This book is dedicated to some questions of theory and practice of the creation of high-current betatrons and two-chamber stereobetatrons, operated at present in some scientific institutions and in the enterprises of the country. During the writing of the book

in essence there is used the original material, obtained by the authors during the calculation, planning and the installation of the operating high-current betatrons and stereobetatrons.

Due to the limited size of the book there is not given the description of other types of the high-current accelerators the information about which appeared recently in the literature.

INTRODUCTION.

At present accelerators are extensively used not only in the scientific investigations in nuclear physics, but also in the medicine - for the treatment of malignant swellings, in biology - for the study of the effect of radiation/emission on the vegetable and animal organisms, including man, in the industrial flaw detection - for nondestructive inspection of large-size and thick-walled articles and materials, in machine building - for the high-speed/high-velocity photograph of the fast-moving machine parts and mechanisms, in physics and chemistry - for the high-speed/high-velocity photograph of the rapidly elapsing physical and chemical processes, and in many other regions.

Because of simplicity of construction/design and maintenance/servicing widest acceptance obtained the induction electron accelerator - betatron. At present in different countries of peace/world work about 200 betatrons, moreover the majority of betatrons is utilized in industrial flaw detection and clinical medicine. A smaller number of betatrons is applied for the scientific investigations in the region of physics, chemistry, etc.

In proportion to the introduction of accelarators into the national economy the requirements fcr them are steadily raised. In this case one of the main requirements, presented now to all accelerators without the exception/elimination, including to the betatrons, consists of an increase in the accelerated current. For the betatron this indicates a sharp increase in the rate cf the dose of the bremsstrahlung, generated by accelerator.

Page 5.

The relatively low intensity cf the radiation/emission of betatrons limits their field of application, since for conducting of many contemporary experimental investigations are required the beam currents of accelerators, to one - three orders exceed the currents, obtained at present. Therefore almost in all laboratories, which carry out by the development cf new ones and by the operation of the existing accelerators, focus special attention on possibility increases in the accelerated current.

An increase in the number cf accelerated particles and, therefore, intensity of the radiation/emission of betatron even two or three times represents the serious problem, during solution of

which are encountered the definite difficulties of technical character. The task of an increase in the accelerated current by two or three orders is considerably more complicated. It requires the preliminary theoretical development of a question and unavoidably leads to qualitative changes of entire accelerator as a whole.

An increase of the current of the charged/loaded particles in the betatron can be achieved/reached by a substantial change in some basic parameters of accelerator.

1. Increase in region of focusing forces of controlling magnetic field of betatron and respectively practical implementation of this magnetic field which would be capably hold down/retain in orbit necessary electronic charge to end/lead of cycle of acceleration. An increase in the region of the focusing forces leads to the appropriate increase in the interpole space of betatron. With the considerably larger sizes/dimensions of the aperture of accelerator it is necessary to apply the new principles of the calculation of magnetic field and profile/airfoil of the pole pieces, since the usual calculation methods prove to be unsuitable, since some approximations/approaches, for example the straightness of the lines of force of magnetic field in the gap of betatron, cannot be accepted for calculating the high-current betatron. Furthermore, the large circulating current of electrons creates sufficiently strong proper

magnetic field, which alsc must be taken into consideration during calculatics of high-current betatrcn.

2. Considerable increase in quantity of electrons, intrcduced intc accelerative dcughnut for guaranteeing calculated circulating current in orbit of accelerater. Here fundamental difficulty consists of the development of the electrcn source, capable of ensuring the high currents of emissicn with the minimal sizes of the working surface of emitter and under the ccndition of high stability and large service life of source.

Page 6.

3. Ccnsiderable increase in wave energy of electrons, with which they are introduced in acceleratien, for guaranteeing most optimum conditions for acceptance in acceleration of necessary number of electrons. In accordance with the theory of inductive acceleration and the experimental data a maximum number of particles, seized into the acceleration, unlimitedly grows/rises with an increase in the energy of the injection of electrons. Therefore upper boundary of the voltage of injection is determined only by the technical considerations, connected with dielectric strength of the structural elements/cells of injector. Difficulty with the resolution of the problem of high-voltage injection consists of the development of

system which would allow ten times to at least increase energy of the introduction/input of electrons in the acceleration, accepting with respect to the attention the limitedness of space for the arrangement/position of the parts of injector, which are located under the high pulse potential. Furthermore, the development stable working pulse generator of the voltage of the specific form in amplitude into hundreds of kilovolts and duration several microseconds represents a rather serious task.

4. Change of conditions for acceptance of electrons into acceleration, capable of leading to increase in seized and finished to end/lead cycle of acceleration of number of electrons. This can be an improvement in the optic, optics of injector, the use/application of a different kind of the contractors, which lead to compression of the instantaneous orbits of electrons at the moment of injection, or the replacement of the existing oscillatory mechanism of capture new, oscillation-free. A change in conditions for acceptance is connected with conducting of labor-consuming and thin experiments with the electron beam into initial period of the cycle of acceleration with a simultaneous change in the parameters of injection and injector. The creation of the new mechanism of capture, for example oscillation-free, meets with the great difficulties of theoretical and, mainly, experimental character. Oscillation-free capture of electrons, based on the spiral accumulation, is realized and

convenient upon the internal injection and with the relatively low voltage. The use of this mechanism upon the external injection and with the voltage into several hundred kilovolts is virtually impossible.

Page 7.

5. Essential shortening of duration of pulse of radiation when it is necessary to obtain maximum pulse current of accelerated electrons to target. In the betatron with the ample clearance shortening the duration of emission impulse represents serious technical task because of the need to displace the large ring current of relativistic electrons for the fractions/portions of microsecond up to the distance of 200-250 mm in the radial direction. For the solution of this problem is necessary the special inertia-free (low-induction) system, capable of generating the pulse magnetic fields of short duration in the interpolar space of betatron.

6. Increase in current frequency, feeding the accelerator, for obtaining high average/mean rate of dose of bremsstrahlung of betatron. However, an increase in the frequency is accompanied by a sharp increase of the losses in steel of magnetic circuit and requires gain in weight and dimensions of installation as a whole. Therefore, in each specific case a question of the selection of the

operating frequency of the feeding betatron current is solved, on the basis of the permissible dimensions, weight and installation charge, on one hand, and from the required radiation dose rate - on the other hand.

In NII [НИИ - Scientific Research Institute] nuclear physics of Tomsk polytechnic institute were carried out the theoretical studies, dedicated to the theory of capture of electrons in the acceleration and to obtaining the large circulating current of electrons in the betatron, and also experimental design and physical engineering developments for obtaining the high currents of particles, accelerated in the betatron, and therefore the high rates of the doses of the bremsstrahlung of induction accelerators. Both in the USSR and abroad these works served as base for the creation of the first high-discharge betatrons of industrial designation/purpose in the range of energies 15-25 MeV in which the accelerated current into hundreds of times exceeds the currents, obtained in the usual betatrons.

Chapter 1.

THEORETICAL FUNDAMENTALS OF OBTAINING HIGH CURRENTS IN THE BETATRON.

Magnetic field and electromagnet.

An increase in the current of the particles, accelerated in the betatron, is connected, first of all, with an increase in the space of the working zone of betatron, i.e., with an increase in space of the V area of action of the focusing forces S. With the assigned magnitude of the focusing forces of magnetic field the steady-state density of electronic charge ρ_0 is a constant value, and in this case the number of particles which can be held down/retained by the field of betatron, it is proportional to space of the V area of action of the focusing forces. For this case $\rho_0 \sim \frac{Q_1}{V_1} = \frac{Q_2}{V_2} = \text{const}$, where Q - charge of the accelerated in the betatron beam; $V=2\pi r_0 S$ - space of the area of action of the focusing forces with a section S region and a radius of the equilibrium orbit r_0.

If charge $Q_2 = 10^n Q_1$, then $\frac{Q_1}{V_1} = \frac{Q_2}{V_2} = \frac{10^n Q_1}{V_2}$, for increase of charge Q 10^n times it is necessary, other conditions being equal, so many times to increase the space of the magnetic field of betatron. An

increase in the volume of magnetic field of betatron is connected with an increase either in the geometric dimensions of interpolar space or radius of equilibrium orbit. Both that and others lead to a sharp increase of dimensions and weight of accelerator and an increase in the consumed electrical energy. Therefore an increase in the interpolar space of betatron should be limited by reasonable limits. A decrease in the sizes/dimensions of the interpolar space of betatron with the prescribed/assigned electronic charge can be obtained, increasing the density of charge ρ_0 at the moment of its introduction/input into the zone of action of the focusing forces. To raise ρ_0 with prescribed/assigned Q is possible only by a increase in the focusing forces of the controlling magnetic field.

Page 9.

but since the forces, which operate on the beam from the side of magnetic field, are proportional to intensity/strength H the fields, then for increase in Q should be introduced electrons into the chamber/camera with large H, i.e., with the larger energy of the injected electrons.

Taking into account this, was acknowledged by advisable increase the area of action of the focusing forces of betatron, i.e., the "capacity/capacitance" of the magnetic field of accelerator

approximately ten times (or somewhat more), which corresponds to the possibility of the proportional increase of the accelerated current of particles in the constant/invariable energy of the injected particles. An increase of the accelerated current of particles 10-15 more times subsequently was obtained as a result of increasing the voltage of the injection of electrons of up to several hundred kilovolts. Theoretical questions of obtaining the guiding field of high-current betatrons were developed by B. N. Rodimov and P. A. Cherdantsev.

§ 1. Potential function V_n - the fundamental characteristic of the controlling magnetic field of betatron.

The region of the focusing forces of the magnetic field of betatron determines the quantity of electrons which can be seized into the acceleration under prescribed conditions of injection. The focusing properties of field are usually rated/estimated by the value of the index of the drop of field n at the different points of the working gap of betatron [1]. However, distribution n does not give the demonstrative picture of the distribution of the focusing field forces. The most completely focusing forces and the quality of the guiding field of betatron characterizes V_n - the potential function of the focusing forces of the magnetic field of betatron. Potential function V_n in a specific manner is connected also with value n.

This connection/communication can be shown as follows.

For the nonrelativistic case tangential component/term of the rate of the electron, which moves in the field of betatron, is expressed in the form

$$v_\theta = \sqrt{\frac{2e}{m} V_u} \qquad (1)$$

Focusing force in the direction of Z-axis

$$m\ddot{z} = -e\frac{\partial V_u}{\partial z} = \frac{e}{c} v_\theta H_r \qquad (2)$$

whence

$$H_r = -\frac{1}{\sqrt{2V_u}} c \sqrt{\frac{m}{e}} \cdot \frac{\partial V_u}{\partial z} . \qquad (3)$$

The focusing force in direction r

$$m\ddot{r} = -e\frac{\partial V_u}{\partial r} = -\frac{e}{c} v_\theta \Delta H_z \qquad (4)$$

whence

$$\Delta H_z = \frac{1}{\sqrt{2V_u}} c \sqrt{\frac{m}{e}} \cdot \frac{\partial V_u}{\partial r} , \qquad (5)$$

where $\Delta H_z = H_z - H_{z0}$ - difference between the magnetic intensity at the particular point and the strength of field, which is necessary for the electron motion along the circle with radius of r with a speed of v_θ. This difference creates the focusing force in direction r. H_{z0} is found from the relationships/ratios

$$\frac{mv_M^2}{r} = \frac{e}{c} H_{zv}; \quad H_{zv} = \frac{c}{r}\sqrt{\frac{2m}{e} V_M}. \qquad (6)$$

Then

$$H_z = H_{zv} + \Delta H_z = \frac{c}{r}\sqrt{\frac{2m}{e} V_M} + c\sqrt{\frac{m}{e}} \times$$
$$\times \frac{1}{\sqrt{2V_M}} \cdot \frac{\partial V_M}{\partial r}. \qquad (7)$$

[Page 11] Since

$$n = -\frac{r}{H_z} \cdot \frac{\partial H_z}{\partial r}, \qquad (8)$$

then

$$n = 1 - \frac{2\frac{\partial V_M}{\partial r} + r\left[\frac{\partial^2 V_M}{\partial r^2} - \frac{1}{2V_M}\left(\frac{\partial V_M}{\partial r}\right)^2\right]}{\frac{2V_M}{r} + \frac{\partial V_M}{\partial r}}. \qquad (9)$$

In an equilibrium orbit $r=r_0$ (neq) $z=0$; $\frac{\partial V_M}{\partial r}=0$, then

$$n(r) = 1 - r_0^2\left(\frac{\frac{\partial^2 V_M}{\partial r^2}}{2V_M}\right)_{r_0,\,0}. \qquad (10)$$

From condition $\frac{\partial H_z}{\partial r} = \frac{\partial H_r}{\partial z}$ it is possible to obtain the relationship/ratio

$$n(r) = r_0^2\left(\frac{\frac{\partial^2 V_M}{\partial r^2}}{2V_M}\right)_{r_0,\,0}. \qquad (10a)$$

Thus, the examination of the characteristics of the field of betatron on base V_M considers distribution n.

Potential function makes it possible to also calculate the density of equilibrium beam in the betatron. However, in the case of accelerating the large number of particles during calculations it is necessary to consider the field of equilibrium electron beam. The account of the proper field of beam and the computation of the density of equilibrium beam in the betatron it is carried out in work [2]. Relativistic function V_p is examined here in the form of sum $V_p = V_p' - V_p''$, where V_p' - potential function of the free from the charge field: V_p'' - the potential function of the magnetic field of beam.

Page 12.

Value V_p' is taken with an accuracy to standard deviations from the equilibrium radius r_0, i.e.,

$$V_p' \approx V_0 \left[1 + \frac{m_0 c^2 V_{om}}{e V_0^2} (1 - n_0) \frac{x^2}{r_0^2} + \right.$$
$$\left. + \frac{m_0 c^2}{e V_0^2} n_0 V_{om} \frac{z^2}{r_0^2} \right], \qquad (11)$$

where V_{om} - value of nonrelativistic potential function with $r=r_0$, $z=0$; n_0 - value of the coefficient of the drop of magnetic field to $r=r_0$, and $V_0 = \frac{m_0 c^2}{e} \times \sqrt{1 - \frac{2eV_{om}}{m_0 c^2}}$; V_p'' - is written/recorded in the form of series/row with the undetermined coefficients

$$V_p'' = V_0 \left(K \frac{x^2}{r_0^2} + K' \frac{z}{r_0^2} \right) \qquad (12)$$

After the computation of coefficients of K and K' for V_p is obtained expression

$$V_p = V_0 \left\{1 + \left[\frac{m_0 c^2 V_{0M}}{2eV_0}(1-2n_0) + \frac{1}{4}\left(\frac{eV_0}{m_0c^2}\right)^2 - \frac{1}{4}\right] \times \right.$$
$$\times \frac{x^2}{r_0^2} + \left[\frac{m_0 c^2 V_{0M}}{eV_0^2} n_0 - \frac{1}{4}\left(\frac{eV_0}{m_0c^2}\right)^2 - \frac{1}{4} - \right.$$
$$\left. \left. - \frac{m_0 c^2 V_{0M}}{2eV_0^2}\right] \frac{z^2}{r_0^2} \right. . \qquad (13)$$

Thus, V_p taking into account the proper magnetic field of beam gives the focusing force which is more than force without the proper field f_r and f_z once for r- and z - directions respectively, where

$$f_r = 1 + \frac{KeV_0^2}{m_0c^2 V_{0M}(1-n_0)}; \quad f_z = 1 + \frac{KeV_0^2}{m_0 c^2 V_{0M} n_0}.$$

Let us rate/estimate the density of the beam which can be held down/retained by the field of betatron.

Since

$$\rho = -\frac{1}{4\pi}\nabla^2 V_p; \text{ and } \quad V_p = \frac{m_0 c^2}{e}\gamma,$$

where

$$\gamma = \frac{eV_p}{m_0c^2} = \frac{mc^2}{m_0 c^2} = \frac{E}{E_0},$$

then

$$\rho = -\frac{m_0 c^2}{4\pi e}\nabla^2\gamma. \qquad (14)$$

But for γ we have an equation

$$\nabla^2\gamma = \frac{\gamma}{\gamma^2-1}\left[\left(\frac{\partial\gamma}{\partial r}\right)^2+\left(\frac{\partial\gamma}{\partial z}\right)^2\right]+\frac{\gamma^2-1}{r^2}\gamma. \quad (15)$$

In the center of beam $\frac{\partial\gamma}{\partial r}=\frac{\partial\gamma}{\partial z}=0$, therefore $\nabla^2\gamma_0=\frac{\gamma_0^2-1}{r_0^2}\gamma_0$, where γ_0 - value γ at point $r=r_0$, $z=0$. Then the charge density in the center of the equilibrium beam

$$\rho_0=-\frac{m c^2}{4\pi e r_0^2}[\gamma^2-1]\gamma$$

or

$$\rho_0=-\frac{m_0c^2}{4\pi e r_0^2}\left[\left(\frac{E}{E_0}\right)^2-1\right]\frac{E}{E_0}. \quad (16)$$

At the ultrarelativistic rates $E>>E_0$, then from equation (16) it is obtained

$$\rho_{0\,рел}=-\frac{m_0c^2}{4\pi e r_0^2}\left(\frac{E}{E_0}\right)^3. \quad (17)$$

For nonrelativistic rates $E=E_0+E_{кин}=E_0+\frac{m_0v^2}{2}$, then

$$\rho_{0кин}=-\frac{V_{0\,н}}{2\pi e r_0^2}\left(1+\frac{1}{2}\cdot\frac{v^2}{c^2}\right). \quad (18)$$

Let us compare the calculated charge densities taking into account the proper magnetic field of beam with the densities, found without its account. The charge densities for the last case are calculated from the following formulas, obtained from the equation of the free from the charge magnetic field:

$$\rho_0'=-\frac{m_0c^2}{4\pi e r_0^2}\left(\frac{\gamma_0^2-1}{\gamma_0}\right)=-\frac{m_0c^2}{4\pi e r_0^2}\cdot\frac{\left(\frac{E}{E_0}\right)^2-1}{\frac{E}{E_0}}. \quad (19)$$

For the relativistic case

$$\rho_0'_{\text{рел}} = -\frac{m_0c^2}{4\pi e r_0^2} \cdot \frac{E}{E_0}, \qquad (20)$$

for the nonrelativistic

$$\rho_0'_{\text{нер}} = -\frac{V_{\text{ом}}}{2\pi e r_0^2}\left(1 - \frac{1}{2} \cdot \frac{v^2}{c^2}\right). \qquad (21)$$

Let us determine differences ρ and ρ_0' for both cases:

$$\Delta\rho_{0\,\text{рел}} = \rho_{0\,\text{рел}} - \rho_0'_{\text{рел}} = -\frac{m_0c^2}{4\pi e r_0^2} \cdot \frac{E}{E_0}\left[\left(\frac{E}{E_0}\right)^2 - 1\right]; \qquad (22)$$

$$\Delta\rho_{0\,\text{нер}} = \rho_{0\,\text{нер}} - \rho_0'_{\text{нер}} = -\frac{V_{\text{ом}}}{2\pi e r_0^2} \cdot \frac{v^2}{c^2}. \qquad (23)$$

From equations (22) and (23) it is evident that in the relativistic case during the computation of the charge density it is necessary to consider the proper magnetic field of beam. At the nonrelativistic rates (when $v/c \ll 1$) the difference between $\rho_{0\,\text{нер}}$ and $\rho_0'_{\text{нер}}$ is small, and the use of formulas, which do not consider charge, is admissible.

Thus, the proper magnetic field of beam plays the significant role at high velocities of electrons. The charge density depends on energy of electrons as E^3. This dependence can explain the behavior of the maximum of the intensity of radiation/emission at the

different values of energy of injection $E_{инж}$. For the concrete/specific/actual betatron the space, occupied by beam with different ones $E_{инж}$, can be considered constant. Then the intensity is proportional to ρ_0, if we by $E_{инж}$ understand energy of electron during the injection. With low energies of injection the intensity is proportional $E_{инж}$, with the large ones - $E^3_{инж}$. Hence ensues/escapes/flows out the need of increasing the voltage of injection in betatron, if is required a considerable increase of the number of accelerated in the installation particles.

Page 15.

§ 2. Equation of the magnetic field of betatron and its use/application for calculating the field.

Let us record equation (9) in the form

$$\frac{\partial^2 V_м}{\partial r^2} - \frac{1}{2V_м}\left(\frac{\partial V_м}{\partial r}\right)^2 + \frac{1+n}{r}\cdot\frac{\partial V_м}{\partial r} - (1-n)\frac{2V_м}{r^2} = 0. \qquad (24)$$

During the known distribution n and prescribed/assigned z according to equation (24) it is possible to find dependence $V_м$ on r.

A similar equation can be obtained, also, for dependence $V_м$ on z with prescribed/assigned r. Differentiating relationships/ratios

(3) and (7) and considering that $\partial H_z/\partial r=\partial H_r/\partial z$, we obtain

$$\frac{\partial^2 V_м}{\partial z^2}-\frac{1}{2V_м}\left(\frac{\partial V_м}{\partial z}\right)^2-n\left[\frac{2V_м}{r^2}-\frac{1}{r}\cdot\frac{\partial V_м}{\partial r}\right]=0. \quad (25)$$

Storing/adding up the left sides of equations (24) and (25), we have

$$\frac{\partial^2 V_м}{\partial r^2}+\frac{1}{r}\cdot\frac{\partial V_м}{\partial r}+\frac{\partial^2 V_м}{\partial z^2}-$$
$$-\frac{1}{2V_м}\left[\left(\frac{\partial V_м}{\partial r}\right)^2+\left(\frac{\partial V_м}{\partial z}\right)^2\right]-\frac{2V_м}{r^2}=0. \quad (26)$$

Equation (26) is the equation of the magnetic field of betatron, which encompasses all fundamental properties of field.

Potential function for the electrons with any value by the constant C, characterizable energy of the electron, which moves in the field of the action of the focusing forces, is written/recorded in the form

$$V_{мC}=\frac{e}{2mc^2}\left[\frac{\frac{rH_z}{2}+C}{r}\right]^2. \quad (27)$$

This equation can be expressed through potential function $V_{м0}$ for "zero electrons" (C=0 $V_{м0}=\frac{e}{2mc^2}\left(\frac{rH_z}{2}\right)^2$ in the form

$$V_{мC}=\left[\sqrt{V_{м0}}+\frac{C}{r}\sqrt{\frac{e}{2mc^2}}\right]^2. \quad (28)$$

Page 16.

Therefore for calculating the field of sufficient to find the solution of the equation of field with C=0. Function $V_{м0}$ can be

expressed through vector potential A:

$$V_{w0} = \frac{eA^2}{4mc^2}. \qquad (29)$$

Substituting in the equation of field value A for V_{w0}, we obtain equation for A:

$$\frac{\partial^2 A}{\partial r^2} + \frac{1}{r}\cdot\frac{\partial A}{\partial r} + \frac{\partial^2 A}{\partial z^2} - \frac{A}{r^2} = 0. \qquad (30)$$

Equation (30) is solved by separation of variables. Assuming/setting $A=U(r)W(z)$, we obtain two equations:

$$\frac{d^2W(z)}{dz^2} = k^2\,W(z), \qquad (31)$$

$$\frac{d^2U(r)}{dr^2} + \frac{1}{r}\cdot\frac{dU(r)}{dr} + \left(k^2 - \frac{1}{r^2}\right)U(r) = 0. \qquad (32)$$

Condition $dW/dz=0$ with $z=0$ gives

$$W(z) = \mathrm{ch}(kz). \qquad (33)$$

Solution of the second equation

$$U(r) = A_0[aJ_1(kr) + bN_1(kr)], \qquad (34)$$

where $J_1(kr)$ and $N_1(kr)$ - the Bessel function and first-order Neumann. The obtained solutions are utilized for calculating the field. We accept as the boundary conditions $n=n_0$ on radius $r=r_0$ of equilibrium orbit and $A=A_0$ on this radius. We propose also that A_0 is minimal on this radius. Then

$$\left.\begin{aligned} aJ_1(kr_0) + bN_1(kr_0) &= 1;\\ aJ_1'(kr_0) + bN_1'(kr_0) &= 0;\\ k^2 &= \frac{n_0}{r_0^2} \end{aligned}\right\} \qquad (35)$$

Latter/last expression is obtained from equation (10a) [1].

FOOTNOTE [1]. From equation (10a) we have $\frac{\partial^2 V_м}{\partial z^2} = \frac{2V_м n_0}{r_0^2}$. Replacing $V_м$ on A, we obtain

$$\frac{\partial^2 A}{\partial z^2} = \frac{n_0 A}{r_0^2} = k^2 A, \text{ i.e. } k^2 = \frac{n_0}{r_0^2}.$$

ENDFOOTNOTE.

Amplitudes a and b can be determined from the equations

$$\left.\begin{aligned} aJ_1(\sqrt{n_0}) + bN_1(\sqrt{n_0}) &= 1; \\ aJ_1'(\sqrt{n_0}) + bN_1'(\sqrt{n_0}) &= 0. \end{aligned}\right\} \qquad (36)$$

Plotted function is constructed according to the formula, obtained for $V_{м0}$ from relationships/ratios (34) and (35):

$$V_{м0} = \frac{eA_0^2}{2mc^2} \operatorname{ch}^2(kz)[aJ_1(kr) + bN_1(kr)]^2. \qquad (37)$$

It is considered that A_0 for the specific case remains constant, i.e., actually expression for $V_{м0}$ takes the form

$$\frac{V_{м0}}{eA_0^2/2mc^2} =$$

$$= \operatorname{ch}^2(kz)[aJ_1(kr) + bN_1(kr)]^2. \qquad (38)$$

Since the potential function has a minimum in region r_0 both in r-

and in z-directions, these graphs are frequently called potential wells. First calculate pits with z=0, then is constructed section along the axis z with $r=r_0$. By the essential characteristic of pit is the area of its section radial plane, i.e., area, included by equipotential, which passes at the level of the apex/vertex of the barrier of pit. The section of tetatron doughnut must wholly encompass this area. For the construction of any equipotentials is taken the fixed value of the potential:

$$V_{\text{вол}} = \frac{e}{2mc^2} A_1^2 = B_1. \qquad (39)$$

[Page 18.] The corresponding value of vector potential will be:

$$A_1 = \sqrt{\frac{2mc^2}{e} V_{\text{вол}}} - \sqrt{\frac{2mc^2}{e} B_1} = A_0 \operatorname{ch}(kz)[aI_1(kr) + bN_1(kr)], \qquad (40)$$

hence

$$\operatorname{ch}(kz) = \frac{A_1}{A_0[aJ_1(kr) + bN_1(kr)]}. \qquad (41)$$

Then the equation of equipotential line

$$z = \frac{1}{k} \operatorname{Arch} \frac{A_1}{A_0[aJ_1(kr) + bN_1(kr)]}. \qquad (42)$$

As the theoretical profile of pole is taken the equipotential, designed from the formula

$$\frac{\operatorname{sh}(kz)}{\operatorname{sh}(kz_0)} = \frac{aJ_0(kr_0) + bN_0(kr_0)}{aJ_0(kr) + bN_0(kr)}. \qquad (43)$$

Line is carried out in such a way that the region of the focusing forces would be completely encompassed by the interpolar space of betatron. Fig. 1 depicts over the long term the potential function (potential well). The calculated values of this function and the theoretical profile of pole are given in Fig. 2. For r_0=23.7 cm and n=0.5 value of values a, b and k they are equal to with respect 1.513, 0.455 and 0.0298.

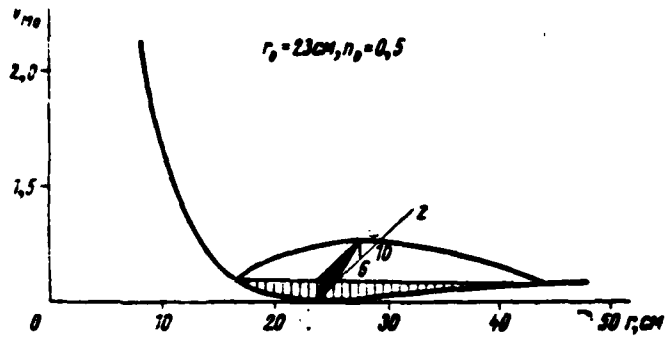

Fig. 1. Potential well of betatron.

Page 19.

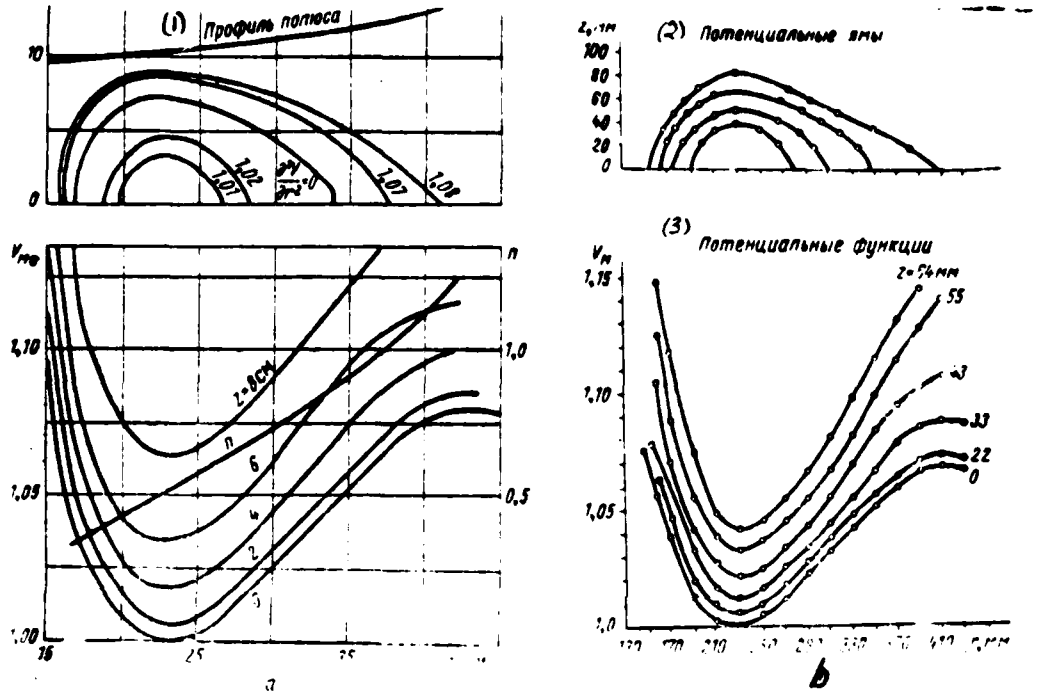

Fig. 2. Calculated (a) and experimentally obtained (b) characteristics of magnetic field of betatron.

Key: (1). Profile/airfoil of pole. (2). Potential wells. (3). Potential functions.

Page 20.

Functions were calculated for z=0; 2; 4; 6 and 8 cm. According to such graphs are constructed equipotential lines, which are

determining the boundaries of the region of the focusing forces (or capture region) and the boundaries of the zone of the maximum equilibrium charge of beam. The theoretical profile of pole is designed for the poles of an infinite radius. Therefore in the manufactured poles it is necessary to experimentally determine the layout of peripheral part for the compensation for the distortions in the distribution of magnetic field along the radius, caused by magnetic leakage fluxes.

§ 3. Calculation of charges and currents of high-current betatron.

With known the parameters of the magnetic field of betatron, in particular at the known cross-sectional area of region focusing forces in interpolar space of accelerator, it is possible to calculate the maximum charge of beam and the circulating currents of high-current betatron.

The maximum equilibrium charge of beam is calculated from the formula

$$Q = \frac{E}{2\pi r_0}\left[\left(\frac{E}{E_0}\right)^2 - 1\right]S, \qquad (44)$$

where S - sectional area of the zone of equilibrium beam. For S≈200 cm² and $U_{max} = 300\frac{кв}{\wedge}$ ($E/E_0 = 1.58$) charge will compose $Q = 5.2 \cdot 10^{-6}$ k, which corresponds to a number of electrons $N = Q/e = 3.33 \cdot 10^{13}$. This charge,

led to the end/lead of the cycle of acceleration and discarded to the target, for example, in $2 \cdot 10^{-7}$ s, creates the pulse current, equal to

$$I_{имп} = \frac{Q}{t} = 25{,}8\ a.$$

Circulating in orbit current in this case

$$I_{ц} = \frac{2\pi r_0 S e n_0 V}{2\pi r_0} = \frac{QV}{2\pi r_0} = 836\ a. \qquad (45)$$

results are obtained taking into account the proper magnetic field of bundle.

§4. On the calculation of the profile/airfoil of poles with n(r)=const [3].

In the majority of the operating betatrons index the drops of field n attempt to select by constant within some limits along a radius of pole. In the usual betatron at the low value of the ratio δ_0/r_0 of interpolar gap δ_0 to a radius of the equilibrium orbit r_0 in the calculation is not taken into consideration the curvature of the lines of force of magnetic field in the working zone of accelerator. In the high-current betatron ratio $\delta_0/r_0 \sim 1$; therefore the curvature of the force line disregarded should not be. The approximate computation of the profile/airfoil of poles taking into account the curvature of lines of force is produced as follows. We will consider that the index of the drop of magnetic field does not depend on r and z, i.e.,

$$\frac{\partial}{\partial z}(nH_0) = 0, \qquad (46)$$

then

$$H_r = -nH_z\frac{z}{r}, \qquad (47)$$

but

$$\frac{dr}{dz} = \frac{H_r}{H_z}. \qquad (48)$$

From relationships/ratios (47) and (48) let us find the equation of the line of force of the magnetic field

$$\frac{dr}{dz} = -n\frac{z}{r}. \qquad (49)$$

whence the radius of curvature of the line of force of the magnetic field

$$\rho = \frac{r}{n}\left(1 + n^2\frac{z^2}{r^2}\right)^{3/2}\left(1 + n\frac{z^2}{r^2}\right)^{-1} =$$
$$= \frac{r}{n}\left[1 - n\left(1 - \frac{3}{2}n\right)\right]\frac{z^2}{r^2}.$$

Page 22.

For virtually adopted values of n and with $z/r \leq 1$ the average/mean radius of curvature of the line of force

$$\rho \approx \frac{r}{n}.$$

Magnetic field in the interpolar space can be expressed as

$$H_z(r, 0) = \frac{\Phi_0}{ap}, \qquad (51)$$

where Φ_0 - magnetic-potential difference of the poles of electromagnet, α - angular radian measure, represented by field line boundary by poles. Value n is expressed by the formula

$$n = -\frac{r}{H_z}\cdot\frac{dH_z}{dr}. \qquad (52)$$

from equations (51) and (52) it is possible to determine value of α:

$$\ln \frac{a}{a_0} = -\int_{r_0}^{r} [1 - n(r, 0)] \frac{dr}{r} \qquad (53)$$

with n(r, 0)=const

$$a = a_0 \left(\frac{r}{r_0}\right)^{n-1}. \qquad (54)$$

The vertical coordinate of polar surface can be expressed as follows:

$$z_1(r - a) = \frac{r}{n(r, 0)} \sin \frac{a(r)}{2}, \qquad (55)$$

where

$$a = \frac{r}{n(r, 0)} \left(1 - \cos \frac{a(r)}{2}\right).$$

Expression (55) together in (53) is called the equation of the profile/airfoil of poles. According to formulas (55) and (53). it is possible to calculate the profile/airfoil of the poles of high-current betatron, also, in the case changing from radius n, if this change is sufficiently steady.

Page 23.

In this case it is assumed that n virtually does not depend on z in the working zone of accelerator. The profile/airfoil of pole for n(r)=const is concave, whereas for n, which grows with r, it is convex. Concave profile/airfoil is more convenient in form, since into the gap with such poles is placed well accelerative chamber/camera. With the convex profile/airfoil of cavities

accelerative chamber/camera more badly is entered in the aperture of betatron. Both versions of profile/airfoil prove to be equivalent from the point of view of the maximum accelerated number of electrons, since the space of the region of the focusing forces with n(r)=const virtually remains the same or somewhat greater, as for case of dn/dr>0.

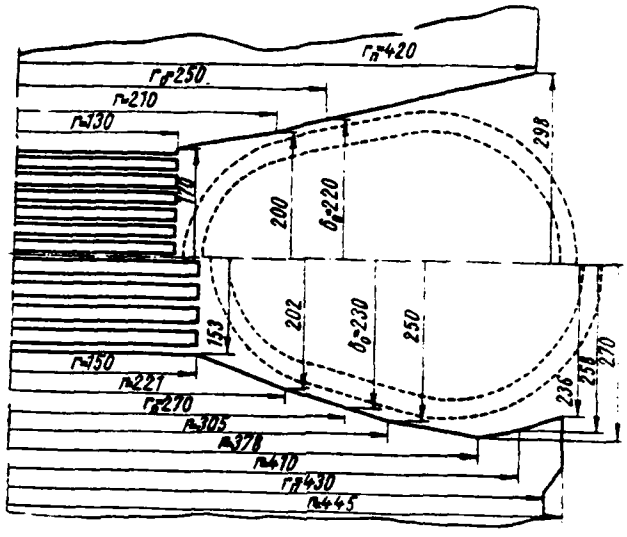

Fig. 3. Two versions of the profile/airfoil of the poles of the high-current betatron: r - a radius of pole; r_0 - radius of equilibrium orbit; r - radius of the fracture of the profile/airfoil of pole; δ_0 - gap on a radius.

Page 24.

Fig. 3. show two versions of the profile/airfoil of the poles which we utilized in the high-current betatron on 25 MeV. The upper profile/airfoil corresponds increasing on radius n, lower - n(r)=const. The diameter of central inserts/bushings in the second case was somewhat increased for increasing maximum energies of the accelerated electrons.

Thus, the aperture of high-current betatron and respectively the cross section of vacuum chamber they are obtained approximately/exemplarily by an order more than in an ordinary betatron to the same energy.

Page 25.

Chapter 2.

HIGH-VOLTAGE INJECTION OF ELECTRONS INTO A CHAMBER OF A HIGH-CURRENT BETATRON.

§5. Identification of the parameters of the pulse of the voltage of injection for the high-current betatron.

Maximum equilibrium electron charge, held by the magnetic field of betatron, is calculated from formula (44), from which it follows that the voltage of injection does not have optimum value for obtaining the maximum accelerated current. The real finite quantity of current is determined by limit on space charge, which has concrete/specific/actual value for prescribed/assigned E. With the growth of E this limit is crowded large Q. Therefore the limit of injection is caused only by technical and economic considerations.

In the majority of the operating betatrons is applied the propagated construction/design of an injector of Kerst's type with the voltage of injection on the order of 40-50 kV. When selecting of the voltage of injection for the high-current betatron on 25-30 MeV

is expedient to raise energy of injection approximately/exemplarily ten times, i.e., to accept $E_{инж}$ = 400 keV. With this voltage the sizes/dimensions of the system of injection as a whole do not leave the reasonable limits and is provided necessary dielectric strength of devices/equipment by usual electrical materials. This increase in the energy of injection gives an increase in the radiation yield more than by an order, other conditions being equal. For a betatron operating on 15 MeV $E_{инж}$ it was respectively selected equal to 200 keV. An increase in the voltage of injection is desirable for decreasing the probability of the shift of operating point from the prescribed/assigned value (with n=0.6) to the nearest dangerous resonance.

Page 26.

Change dn in the effective value of the index of the drop of the magnetic field, created by space charge of bundle, is determined by the relationship/ratio

$$dn = \frac{Qe r_{эл} c^2}{4\pi a^2 E} \left(\frac{1-\beta^2}{\beta} \right), \qquad (56)$$

where Q - charge of the accelerated bundle; a - radius of bundle; E - energy of particles in the bundle ev/c. From expression (56) it is clear that with an increase in the energy of particles upon injection dn is proportionally decreased, therefore, is decreased the shift of

the operating point of accelerator from the prescribed/assigned value.

An increase in the energy of the injected electrons is accompanied by an increase in the radiation yield of the betatron as a result of the reduction of the losses of particles on the atoms of residual gas, due to the relative decrease of the effect of magnetic bumps, etc. Thus, only increase $E_{инж}$ with the constant/invariable to the point of injection $I_{инж}$ leads to the specific increase in the intensity of radiation/emission. However, the fundamental effect of an increase in the accelerated current with larger $E_{инж}$ is connected with the increase of density ρ_0 of the equilibrium charge of bundle in the zone of the focusing forces of betatron. This means that into accelerator chamber with large E can be introduced a respectively larger number of electrons with the total charge Q. Consequently, with an increase in the voltage of injection it is necessary in the required proportion to increase injected into the chamber/camera electronic current $I_{инж}$. In works [4, 5] it is shown that current $I_{инж}$ with increase $E_{инж}$ grows/rises nonlinearly:

$$I_{пред} \approx \frac{1}{4} (\beta\gamma)^3 \frac{\frac{R_c}{r_0}}{\ln \frac{R_c}{R_и}} I_0, \qquad (57)$$

where β, γ - relativistic factors of the injected bundle; R_c - given radius of the cross section of region the focusing forces; $R_и$ -

initial radius of bundle; r_0 - radius of equilibrium orbit; I_0 - constant, equal to $17 \cdot 10^3$ to a.

Page 27.

As is evident, the current of injection increases proportionally $(\beta\gamma)^3$. This value can be recorded in the form $(\gamma^2-1)^{3/2}$, whence it follows that dependence I_{max} on E_{max} is analogous the dependence of the intensity of radiation/emission on E_{max}, which from the linear dependence with small ones E_{max} passes into the cubic with large ones E_{max}.

Such by shape, an optimum increase in the intensity of radiation/emission by increase E_{max} is achieved only with the appropriate increase in the current of injection.

The duration of the interval of capture of electrons τ_3 at acceleration is evaluated differently and as a rule, do not exceed 0.5 μs, which corresponds to 50-100 turns of electrons on the orbit. There are indications that this interval can correspond in all to several turns. With multiturn injection, which is commonly used in the betatrons, the duration of the pulse of the voltage of injection t_{max} always considerably more than the duration of interval τ_3 varies for the different accelerators in the range from 1.5 to 10 μs.

The duration of injection pulse in the limits from 1.5 to 3 μs it is possible to consider completely of a sufficient and for the case multiturn high-voltage injection in the high-current betatrons.

Should be also examined a question about the pulse sinchronization of the voltage of injection (relative to the level of magnetic field) with the large amplitude of current. The impulses/momenta/pulses of negative voltage, supplied to the cathode of electron gun, are generated by the special diagram of injection. Energy of the electrons, introduced into accelerator chamber, it is necessary to match with a value of magnetic intensity in orbit and its radius. The quantitative connection/communication between these values in the nonrelativistic case is determined by the condition of the injection

$$t_{инж} = \frac{3{,}37\sqrt{U_{инж}}}{r_0 H_0 \Omega}, \qquad (58)$$

where $t_{инж}$ - moment/torque of injection, calculated off the moment/torque of transiting the magnetic flux through the zero value, μs; $U_{инж}$ - the voltage of injection, in; H_0 - magnetic intensity in orbit of radius r_0, oerst.; Ω - angular frequency of the feed of the electromagnet of betatron.

From condition (58) it follows that voltage and the moment/torque of injection must be matched with the design parameter of accelerator (H_0, r_0, Ω_0). This agreement is acccmplished/realized by a change in mcment/torque or voltage of injection. Since for obtaining the maximum intensity of radiation/emission we attempt tc work with the largest possible voltage of injection, then the fundamental controlled parameter must be the mcment/torque (phase) of injection. The required precision/accuracy of the pulse sinchrcnization of injection relative to the level of magnetic field in orbit depends on the parameters of the magnet of betatron and cn the parameters of the impulse/momentum/pulse of injection. The precision/accuracy of synchronization in the time units can be expressed as follows. Let us assume that the input time of electrons in orbit of betatron is known and it is equal approximately tc 1 μs. Then with a precise constancy of the amplitude of the ceiling voltage and strength of field in orbit it is possible to allow time scattering of 0.1 μs (10o/o of entire input time). In actuality the amplitude of ceiling voltage and the amplitude of field in orbit will, as a result of one or the other reasons, test/experience divergences. It is of interest to rate/estimate the degree of accuracy with which it is necessary to support the constancy of these values.

The condition of injection (58) can be recorded in the form

$$U = KH_{м}^{2} t^{2}, \qquad (59)$$

where K - proportionality factor, which includes constant values r_0 and Ω; U - voltage of injection; $H_м$ the amplitude of magnetic intensity at the moment of injection t. Differentiation gives

$$dU = 2KH_{м}^{2} t\,dt + 2KH_{м} t^{2}\,dH_{м}. \qquad (60)$$

After dividing expression (60) on (59), we will obtain

$$\frac{dU}{U} = 2\frac{dt}{t} + 2\frac{dH_{м}}{H_{м}}, \qquad (61)$$

or, passing to the finite difrerences,

$$\frac{\Delta U}{U} = 2\frac{\Delta t}{t} + 2\frac{\Delta H_{м}}{H_{м}}. \qquad (62)$$

Page 29.

Taking into account that the divergences of values can be into both sides, expression (62) should be recorded in the form

$$\pm\frac{\Delta U}{U} \pm \frac{2\Delta t}{t} \pm \frac{2\Delta H_{м}}{H_{м}} = 0 \qquad (63)$$

With the voltage of injection on the order of 300-400 kV for the betatron on 25 MeV (r_0=24 cm) the time lag of the moment/torque of injection relative to the moment/torque of zero-field (phase of injection) composes value on the order of 100 μs (it is more precise than 87 μs). Hence it follows that with $\Delta H_м/H_м = 0$ and $\Delta U/U = 0$ and the assumption of time scattering of 0.1 μs with the input time, equal to

1 μs, $\Delta t/t=0.1$c/c. With the divergence of all values resultant error must not exceed this value (0.1c/c). Then in the worse case

$$\frac{\Delta U}{U}+2\frac{\Delta t}{t}+2\frac{\Delta H_{м}}{H_{м}}\leqslant 0{,}001. \qquad (64)$$

During the use of the modern delay circuit it is possible to ensure precision/accuracy $\Delta t/t=0.1$c/c. From inequality (64) it is evident that this precision/accuracy can be observed only with $\Delta U/U=0$ and $\Delta H_{м}/H_{м}=0$. With the high energies in the extreme relativistic case is correct the expression

$$U=300H_{r},$$

from which analogously it is possible to obtain relationship/ratio (assuming that $H=H_{м}\sin\omega t$ and ω=const)

$$\frac{\Delta U}{U}+\frac{\Delta H_{м}}{H_{м}}+\frac{\Delta t}{t}\leqslant\varepsilon, \qquad (65)$$

where ε - low value.

From inequality (65) it follows that in the relativistic case of requirement for the precision/accuracy the constancies of values descend. For us greatest interest is of the intermediate velocity band of electrons, in which the amplitude of field and time lag are connected with the relationship/ratio

$$U=\sqrt{0{,}26+(3rH_{м0})^{2}\sin^{2}\omega t\cdot 10^{-8}}-0{,}51, \qquad (66)$$

where U - voltage (amplitude) of injection, MeV; $H_{м0}$ - amplitude of magnetic field in orbit, G, r - radius of orbit, cm; ω - angular

frequency, rad/s.

Page 30.

The connection/communication between the errors in this case will be more complicatedly; however, for the practical calculations it is possible to use inequality (64), which gives a somewhat increased on the precision/accuracy result.

In usual betatrons by 15-25 MeV, working at the frequency 50 Hz, the requirements for the precision/accuracy of constancy of values somewhat descend, but it is insignificant. However, experiment shows that in the majority of the cases easily is reached the satisfactory work even at the oscillation/vibration of line voltage within limits of 2-3o/o. This is explained by the fact that in the betatron can be created the conditions for the automatic fulfillment relationships/ratios (63) as a result of three factors. The commutating instrument of the diagram of injection is started usually by the voltage pulse from the peaked-wave device (picker).

The shape of the pulse of the voltage of this sensor with an increase of the amplitude of alternating current in the field coils of magnet charges so that the impulse/momentum/pulse becomes narrower, and its amplitude increases. If we assign the specific

level of functioning, then it is possible to obtain the automatic decrease of the pulse delay of the voltage of injection with the increase of field. To this contributes also a corresponding increase in the amplitude of the voltage of injection with the increase of line voltage, which leads, in turn, to the earlier functioning of the diagram of injection with the insufficiently steep wave front of the igniting impulse/momentum/pulse on the grid of the commutating instrument. However, the role of the second factor is small in comparison with the first. The nonstabilized bias voltage attempts, on the contrary, to increase delay in the case of the increase of line voltage. During the specific combination of these three factors it manages via the series/row of the tests/samples to obtain automatic mutual compensation and, therefore, the relatively stable operation of betatron. But even during this selection betatron works insufficiently stably, the insignificant "drift" of the parameters causes the fluctuations of the average/mean radiation level in the large range, which requires the continuous tuning of betatron in the process of work.

Page 31.

With the large amplitude of ceiling voltage the injections of requirement for the precision/accuracy of synchronization are raised and accordingly are raised requirements for the electronic

synchronizing units. The insufficiently good precision/accuracy of synchronization can lead to the high expenditures of time during the adjustment of accelerator for optimum radiation/emission, especially with the work of betatron in the mode/conditions of single impulses/momenta/pulses. On the basis of the aforesaid, requirement, they are presented to the high-voltage multiturn system of injection in the high-current betatron, we can briefly formulate as follows.

1. Voltage with which electrons are injected into chamber/camera of accelerator, must be approximately 400 and 200 kV for 25 and 15 MeV of betatron respectively.

2. Current of injection must be order 8-15 A in impulse/momentum/pulse for duration of pulse 1.5-3 μs. Taking into account that the large part of the injected against gun current perishes on the chamber walls and the parts of injector device/equipment, the full current for which should be designed the system of injection, it must be 40-100 a in the impulse/momentum/pulse.

3. To provide possibility of shape control of impulse/momentum/pulse in some limits for investigation of effect of shape of pulse of voltage of injection on capture of electrons in betatron with high energies of introduction/input.

4. Injector device/equipment must give electron beam with small (order of 1-2°) angle of divergence for guaranteeing best conditions for acceptance of electrons in acceleration.

5. Electronic device, which controls moment/torque of cycling electrode voltage of gun, must provide necessary precision/accuracy of synchronization and continuously variable control of phase of injection. The satisfaction of these requirements presents sufficiently more technical difficulties, connected mainly with the guarantee of dielectric strength of the sections of the insulation of injector device/equipment, the elimination of the electrical breakdown of air and vacuum gaps/intervals, limitation of the onset of corona on the high-voltage current-carrying elements/cells of device/equipment, and also with the creation of the high-voltage generator of the large pulse currents whose power reaches several ten megawatts.

Page 32.

is sufficiently difficult also the development of the injector, which makes it possible to obtain electronic currents of the large density, necessary for guaranteeing the required current of injection with the

voltage on the electron gun, that is 200-400 kV.

§6. Oscillator circuit of the high-voltage impulses/momenta/pulses of injection.

There are several possible versions of the oscillator circuit of the pulses of the voltage of the injection:

1. Schematic of discharging the forming line, preliminarily charged/loaded from the source of high voltage to design stress of the primary winding of peak transformer (30-60 kV in the case of high-current betatrons) through the commutating elements/cells of the type of the controlled discharger/gap with the high stability of the functioning, which ensures the commutation of current in amplitude 1.5-2 kV with the work in the mode/conditions of single impulses/momenta/pulses and with f=50 Hz or special gas-discharge lamp (for example, hydrogen thyratron TGI-2500/35).

2. Diagram, made on modulator tube with full charge of capacity/capacitance and with partial discharge of capacity/capacitance. Diagram makes it possible to regulate the shape of the pulse: the duration of fronts, the drop of flat/plane part, and also its duration.

3. Diagram of transformation of impulses/momenta/pulses with the aid of system of lines with different wave impedance. Possibly also the use/application of cascade transformers or resonator accelerators, which, however, too complicates the system of injection.

The schematic diagram of injection, accepted as the standard for the high-current betatrons, is given in Fig. 4. Diagram works as follows. The capacitors/condensers of the forming line are charged from the charge transformer through the valve/gate, charging resistor and primary winding of peak transformer during the action of the positive wave of voltage. The discharge of the forming line to the primary winding of the peak transformer through the commutating instrument is done when on the anode of valve/gate is the negative potential relative to the "earth/ground". The moment/torque of discharge is controlled by special synchronizing circuit.

Page 33.

In secondary winding of peak transformer appears the narrow pulse of high voltage, supplied to the electrodes of the gun of betatron. With the appropriate phasing the processes in the charge and discharge circuits proceed at the different moments of time, and their duration is sharply different; therefore processes can be examined separately.

The discharge circuit of diagram consists of the accumulator/storage of energy (capacitor/condenser or the forming line), peak transformer and switching device/equipment (electronic, either gas-discharge tube or discharger/gap). The procedure of calculation of the elements of the network of the injection of betatrons is developed by V. M. Razin [6] for the usual betatrons TPI ($U_{max} \approx 60$ kV) and is applicable in essence for the high-voltage injection in the high-current betatrons.

The special feature/peculiarity of the system of injection of high-current betatron lies in the fact that the voltage generator must ensure the stable generation of the very powerful/thick pulses of voltage (40 MW in the impulse/momentum/pulse for the high-current stereobetatron on 25 MeV). This special feature/peculiarity is reflected in constructive solutions during the planning and realization of both separate assemblies and entire generator as a whole.

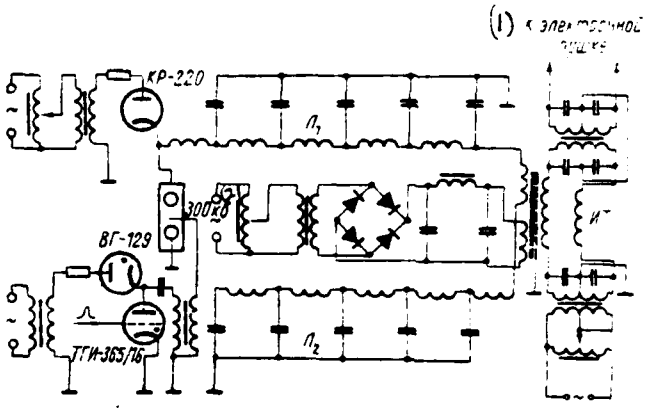

Fig. 4. Schematic diagram of injection for the high-current betatrons.

Key: (1). To the electron gun. (2). kV.

Page 34.

§7. Introduction system of electrons into the chamber/camera of high-current betatron (injector-inflector device/equipment).

Kerst's usual injector allows/assumes the use/application of voltages of injection not more than 100 kV. With more high voltages the use/application of this injector virtually is eliminated due to the insufficiency of dielectric strength of device/equipment. In the high-current betatrons as the injector are applied several types of three-electrode electron guns at the voltage from 200 to 400 kV.

Since the geometric dimensions of gun are sufficiently great, and the elements of construction/design contain the sufficiently large masses of metal, injector is arranged/located beyond the limits of the working zone of the interpolar space of betatron. The carrying out of injector from the working zone of accelerator caused use/application in all cases of special supplementary input equipment - inflector. Inflector is fulfilled in the form of cylindrical capacitor/condenser and is intended for wiring and rotation of the injected by gun bundle tangentially to the instantaneous orbit of electrons at the moment of injection. All developed injector devices/equipment consist of the end-type three-electrode gun, carried out from the working magnetic field of betatron and electrostatic inflector, which leads electron beam into the capture region.

The fundamental elements/cells of electron gun and interelectrode distances preliminarily can be calculated employing the procedure, used for calculating the guns of pier, utilizing the known prescribed/assigned parameters: accelerating anode voltage U_a and beam current I. The design parameters of gun are determined from the following considerations. We will consider that the axially symmetrical electron beam has a section, approximately equal to the emitting surface of cathode S_k. The distance between the anode and the cathode let us designate d. The connection/communication between the current density j, voltage U_a and distance d takes the form of known

"three halves power law":

$$j = A\frac{U_a^{3/2}}{d^2}, \qquad (67)$$

where $A = \frac{4}{9}\varepsilon_0\sqrt{2\eta} = 2{,}33\cdot10^{-6}$; $\eta = e/m$ - charge to mass ratio of electron. Considering system cathode - anode as the parallel-plate capacitor, infinitely extended along the axes x and y, we obtain potential distribution along Z-axis in the form

$$\frac{U(z)}{U_a} = \left(\frac{z}{d}\right)^{4/3}, \qquad (68)$$

where z - distance from the cathode to the point in question; U(z) - potential at this point (on anode z=d). It differentiated expression (68), let us find electric intersity in the plane of the anode

$$E_a = -\frac{4}{3}\cdot\frac{U_a}{d}. \qquad (69)$$

For the compensation for the Coulomb expansion of bundle, emitted by the cathode of finite dimensions, is introduced the focusing electrode in the form of cone with vertex half-angle

$$\theta = \frac{3}{8}\pi = 6{,}75°,$$

by characteristic for all systems of the obeying the law three second. The form of the anode is determined equipotentially electric field $U_1 = U_a$. Virtually the form of the focusing electrode and anode can be simplified. In particular, for the injector of the betatron, into which the introduction/input of electrons into the chamber/camera is accomplished/realized with the aid of the inflector (i.e. the layout of bundle to a considerable degree is determined by

the parameters of inflector, but not by the form of the electrodes of injector), it is possible to allow the use/application of the focusing electrode and anode in the form of flat/plane diaphragm.

Page 36.

The important characteristic of electron beam is perveance p, determined by the relation

$$p = \frac{I}{U_a^{3/2}}, \qquad (70)$$

or microperveance p_μ, determined by equality $p = p_\mu \cdot 10^{-6}$. Since current density $j = I/S_к$, from relationship/ratio (67) we will obtain

$$\frac{I}{S_к} = \frac{2{,}33 \cdot 10^{-6} U_a^{3/2}}{d^2}, \qquad (71)$$

whence

$$\frac{d^2}{S_к} = \frac{2{,}33}{p_\mu}, \qquad (72)$$

and

$$d = 1{,}53 \sqrt{\frac{S_к}{p_\mu}}.$$

Values U_a and I are assigned. Therefore for determining of d it is necessary to know the area of cathode $S_к$. In our injectors cathodes it was made in the form of spirals from the activated tungsten wire, a number of spirals $n_к$. The necessary area of cathode can be tentatively determined, if is known the required current of injection $I_{инж}$ and the

specific emission of electrons from the surface of cathode. Value $S_к$ is determined from the formula

$$S_к = S_{сп} n_к = \frac{S_{сп} I_{нагр}}{I_к} = \frac{I_{нагр}}{AT^2 e^{\frac{1}{T}(4{,}39\sqrt{E} - b_0)}} \text{ см}^2. \quad (73)$$

Here E - intensity/strength of the accelerating electric field in cathode, V/cm; I - current, emitted by cathode; $S_{сп}$ - emitting area of one of $n_к$ the spiral cathodes; T - absolute temperature of cathode; b_0 A - tabular constants from work [7].

For the conclusion/output of electrons from the gun in its anode is made the opening/aperture. The anodic opening/aperture of gun operates on the bundle as the strong diverging lens, as a result of the "sagging" of equipotential surfaces of electric field inside the opening/aperture. Appearing transverse component of electric field deflects electrons from the axis/axle.

Page 37.

For determining the angle of departure the outer beam electrons from the anodic opening/aperture we will use formula for the focal length of thin electronic lens

$$F = \frac{4U_a}{E_1 - E_2}, \quad (74)$$

where E_1 - strength of field to the left of the plane of lens, and E_2

- tc the right (Z-axis is directed from left to right). Apprcximately it is possible to consider that $E_2=0$, and $E_1=E_a$. After substituting expression (69) in (74), we will cttain $F=-3d$. Minus sign indicates the scattering action of the lens whose focus is arranged/lccated to the left of the plane of the ancde. Then the angle of departure of electrons γ_a from the ancdic opening/aperture is determined by the equality

$$\operatorname{tg}\gamma_a = \frac{r_a}{|F|} = \frac{1}{3}\cdot\frac{r_a}{d}, \qquad (75)$$

where r_a - radius of bundle.

Using expression (75), it is possible to determine a radius of bundle r_a after cutput frcm the gun at the prescribed/assigned distance of l from the ancdic diaphragm. If the inflector device/equipment is established/installed at a distance l, then the distance between the inflector plates at the input of beam into the inflector (when into the slot cf the inflectcr device/equipment must enter entire bundle frcm the gun) it is determined by the value cf order $2r_a$.

The parameters of the inflectcr device/equipment are determined from the condition for electron mction along the circular path in the electric field of cylindrical capacitor in the presence of the perpendicularly superimposed weak magnetic field cf betatron. Electrons with a mass cf m_0 and speed v_0, entering into electric

field by intensity/strength E of the cylindrical capacitor, located in the edge/boundary magnetic field of betatron by intensity/strength H, can move over the circular path of radius $r_c = a$ during the selection of the corresponding intensities/strength of electromagnetic field. From the condition of equilibrium of forces which operate on the particles in the field of capacitor, we have

$$\frac{m_0 v_0^2}{a} = \frac{eU_{кон}}{a \ln \frac{R_1}{R_2}} + \frac{ev_0 H}{c}, \qquad (76)$$

where $U_{кон}$ - voltage drop across capacitor plates, and R_1 and R_2 - radii of curvature of capacitor plates.

Under the effect only of one of the fields the radius of curvature for the electric field is determined by the expression

$$a_э = \frac{m_0 v_0^2}{e} \cdot \frac{a \ln \frac{R_1}{R_2}}{U_{кон}}, \qquad (77)$$

but for the magnetic field

$$a_м = \frac{m_0 v_0 c}{eH}. \qquad (78)$$

From these relationships/ratios it follows

$$\frac{1}{a} = \frac{1}{a_э} + \frac{1}{a_м}. \qquad (79)$$

Being given the value of a radius of particle trajectory in the field of capacitor and taking into account the action of magnetic field H, it is possible to calculate the necessary potential difference $U_{кон}$

between the plates of capacitor. Concrete/specific/actual value $U_{кол}$ depends on the distance between the plates of inflector and the angle ϕ, to which it is necessary to turn the injected bundle for its introduction/input into the chamber/camera tangentially to the orbit of injection.

Is obvious, injector device/equipment to the voltage 200-400 kV - not only electron-optical system, but also the high-voltage device/equipment. Therefore during the construction of injector we were directed for the conventional high-voltage constructions/designs, taking into account the special requirements, presented by technical assignment to the separate copies of injectors (limitedness of overall dimensions, the absence of electrical breakdowns on the vacuum gaps/intervals and on by the surfaces of dielectric-insulators, the absence of the corona of lead wires and cables, etc.).

Injector is connected up to the accelerative chamber/camera with the aid of the bellows transition/junction. Inflector is hinged attached to the anode of electron gun.

Page 39.

The special bellows device/equipment, mounted in the back end/face of

electron gun, makes it possible to change the submersion depth of cathode on the focusing electrode and the distance between the focusing electrode and the anode without the deterioration in vacuum in the chamber/camera. Thus, construction/design of injector device/equipment gives the possibility to produce the necessary adjustments of the position of injector and interelectrode gaps/intervals directly on the working betatron during the adjustment of installation to the optimum output of brehmsstralung emission.

Is analogously designed high-voltage injector on 350-400 kV for the pulse betatron on 25 MeV. A difference only in the fact that the inflector is not connected directly with the anode of gun and the insulators of injector have large sizes/dimensions. Usually cathode is manufactured in the form of the tungsten spiral, covered will oxidize thorium. For obtaining the necessary current of injection with high voltages of the introduction/input of electrons were established/installed several spirals, connected in parallel. A quantity of spirals varied from five to twelve. Injector device/equipment provided obtaining the current of injection into several amperes (to the output from the inflector). Is working voltage on the inflector 60 kV. Divergence of beam at the output from the inflector does not exceed 2-4°.

The appearance of the injectors of high-current betatrons and

sterecbetatrons is shcwn in Fig. 5.

The impulse/momentum/pulse of inflector voltage has flat/plane apex/vertex, and its duration exceeds the duration of injection pulse. Under these conditions the adjustment cf betatron to the optimum intensity of radiation/emission proves to be most simple and light. Experience of operating high-current betatrons showed that the voltage pulse on the inflector must somewhat advance the voltage pulse on the injector. In this case is provided stable work of the accelerator. In the usual betatrons the voltage of injection oscillates from 20-30 to 70 kV and up to the moment/torque of putting into operation of the first high-current betatron (in 1960) it does not reach 100 kV. Therefore was carried out the experimental check of the dependence of radiation yield on the voltage of injection [18].

Page 40.

The voltage of injection was measured with the aid of the low-distortion divider into 5000 ohms, which consists of the Nichrome wire with a diameter of 0.1 mm, packed bifilar in the special slots/grooves on the subdivided rod of the fiberglass. With each change the voltages of injection installation adjusted slightly on the optimum operating mode by the adjustment of injection, phase and amplitude of voltage on the inflector and filament current of the cathode of injector.

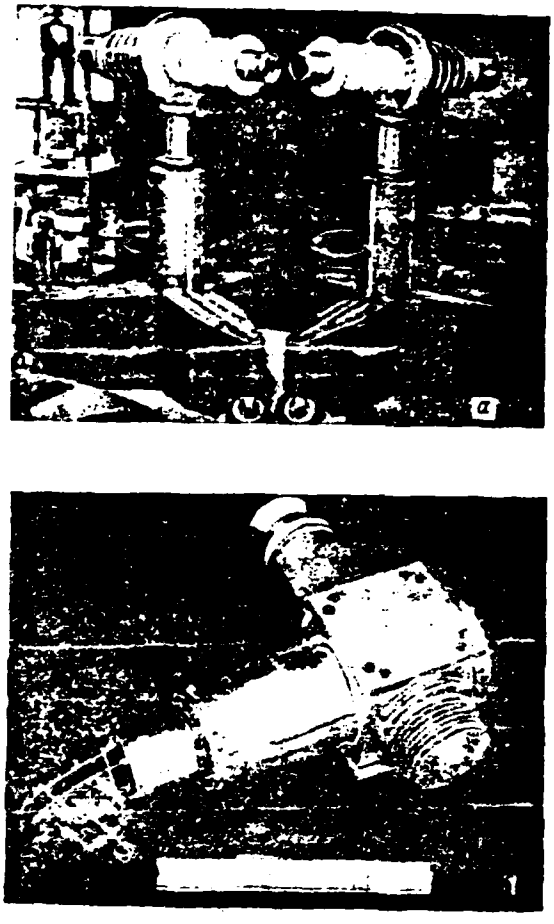

Fig. 5. The general view of injectors to 400 (a) and 200 (b) kV.

Page 41.

The voltage of injection varied with steps/stages on 20-80 kV from 50 to 250 kV. The measurement of the radiation dose rate was made with the aid of ionization chamber by the working volume of 20 cm^3 with

the Plexiglas wall of equilibrium thickness and standard dosimeter of the type "Cactus". Fig. 6 depicts the dependence of the intensity of radiation/emission I_γ in relative unity on the voltage of injection, constructed according tc formula (44). On the graph by small squares are plotted/applied the experimental points, obtained in work [9] with the voltage of injection tc 50 kV. Circles designated the points, obtained by us on the high-current betatron.

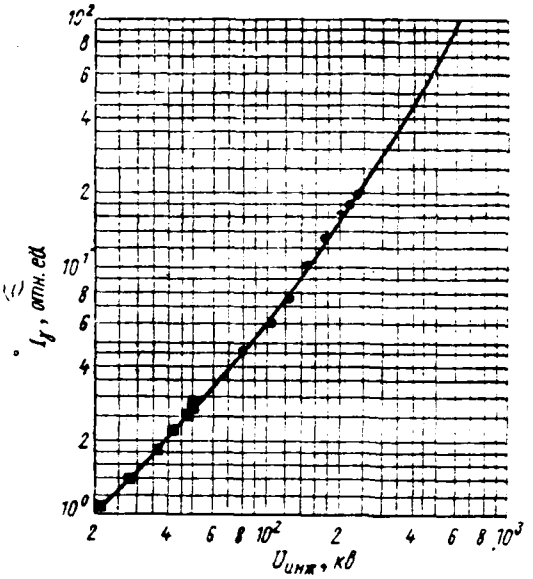

Fig. 6. Dependence of I_γ on the voltage of injection.

Key: (1). rel. un.

Page 42.

The obtained results indicate that to the voltage of injection in 50 kV the intensity of radiation/emission increases in accordance with theory [4, 5], and with voltage, actually utilized in our betatrons, the intensity of radiation/emission increases with growth $U_{инж}$ no longer linear, but to the degree, close to two (it is more precise, is proportional $U_{инж}^{1.8}$). Thus, increase $U_{инж}$ for an increase in the intensity of the radiation/emission of betatron completely

justified itself in practice. The tests of the system of injection on the operating high-current betatrons showed that developed surge generators and injector high-voltage devices/equipment provide the required parameters of the injected electron beam both on the energy and on the current. Is considered by advisable further increase in the voltage of injection in the betatron up to 1000 kV and it is above, where this dependence passes into the cubic. However, by this method appear the considerable technical difficulties, connected with the guarantee of the necessary electrical strength of the system of injection and with obtaining of the high currents of injection.

It is necessary to note also that further increase in the voltage of injection in the betatron makes sense only during the elimination of the lateral instability of bundle, which occurs in the high-current betatron (see Chapter 4).

Page 43.

Chapter 3.

SYSTEM OF SHIFT OF ACCELERATED ELECTRONS FROM EQUILIBRIUM ORBIT TO TARGET.

In the majority of the operating betatrons the shift of the accelerated electrons from the equilibrium orbit to the target is accomplished/realized by the special electronic circuit, which creates one or the other change in the distribution of magnetic fields in the interpolar space of betatron. This change, which leads to the disturbance/breakdown of betatron relation 2:1, is usually achieved by the generation of current pulse in the displacing winding at the discharge through it of preliminarily charged/loaded capacitor bank. Bias coil is arranged/located in the interpolar space of accelerator and depending on the method of the shift of electrons is fulfilled in the different geometric versions. Widest use received those methods of the shifts which lead to the expansion of equilibrium orbit and the "discharge/break" of the accelerated electrons on external target, arranged/located on radius $r_м > r_0$. The

discharge/break of electrons to external target proves to be most desirable for conducting of practical investigations on the betatron. Therefore in the high-current betatrons the shift of the accelerated electron beam was produced predominantly to external target.

The expansion of the orbit of the accelerated electrons can be obtained by two methods: by an additional increase of the magnetic flux in the circle of radius r, i.e., by an increase in the rate of growth of the accelerating magnetic field of betatron, and by weakening magnetic field in an equilibrium orbit. In the first case the electrons acquire supplementary energy due to circuital field of a supplementary increment in the magnetic flux within the orbit and is begun motion along the develcpable spiral to $r_м$, where is arranged/located target. In the second case the energy of electrons remains in effect constant and an increase in the radius of orbit it occurs due to field weakening in operating region of accelerator.

Page 44.

An increment in magnetic flux $\Delta\Phi_0$ required for an increase in the radius of orbit by value $\Delta r = r_0 + r_м$, is determined according to the expression

$$\Delta\Phi_0 = 2\pi H_0 r_0^n \frac{1-n}{2-n}(r_1^{2-n} - r_0^{2-n}), \qquad (80)$$

where H_0 - magnetic intensity on radius r_0; n - index of the drop of

magnetic field. Or

$$\frac{\Delta\Phi_0}{\Phi_0} \approx (1-n)\frac{\Delta r}{r_0},$$

where

$$\Phi_0 = 2\pi r_0^2 H_0. \qquad (81)$$

During the location of turns it is direct on the central inserts/bushings for determining the increment in the induction ΔB_0 in orbit at the moment of the shift, required for change r_0 to value Δr, it is possible to use the analogous expression

$$\frac{\Delta B_0}{B_0} = (1-n)\frac{\Delta r}{r_0}. \qquad (82)$$

If the turns of the displacing winding encompass only the shaped part of the poles, the necessary charge ΔH_0 in the strength of field is determined according to the expression

$$\Delta H_0 = H_0\left[\frac{r_0}{r_1} - \left(\frac{r_0}{r_1}\right)^n\right] \qquad (83)$$

or

$$\frac{\Delta H_0}{H_0} = -(1-n)\frac{\Delta r}{r_0}. \qquad (84)$$

Minus sign indicates weakening of the strength of field with an increase in the radius of orbit.

In the usual betatrons the system of shift, calculated from the given prerequisites/premises, provides the shift of electrons from the equilibrium orbit and the "discharge/break" of them to the target for time $t_{сбр} = (10 \div 20)\cdot 10^{-6}$ s.

In high-current betatrons, the task considerably becomes complicated due to the large sizes/dimensions of air gap and, therefore, because it is necessary to obtain the required increment in the magnetic intensity in the large space. Task even more becomes complicated, if it is necessary to obtain emission impulse by duration $\tau_{имп} = (0.1 \div 0.2) \times 10^{-6}$ s, i.e., by an order is less than $\tau_{сбр}$, usually provided by the system of shift, and, on the contrary, when it is necessary to obtain emission impulse with the duration, which considerably exceeds $\tau_{сбр}$.

§8. Obtaining short emission impulse in the high-current betatron.

The high-current betatron, intended for the high-speed/high-velocity X-ray exposure of the high-speed processes, must generate emission impulse by the duration not more than $0.2 \cdot 10^{-6}$ s. To obtain this duration of emission impulse by the usual methods of shift is impossible.

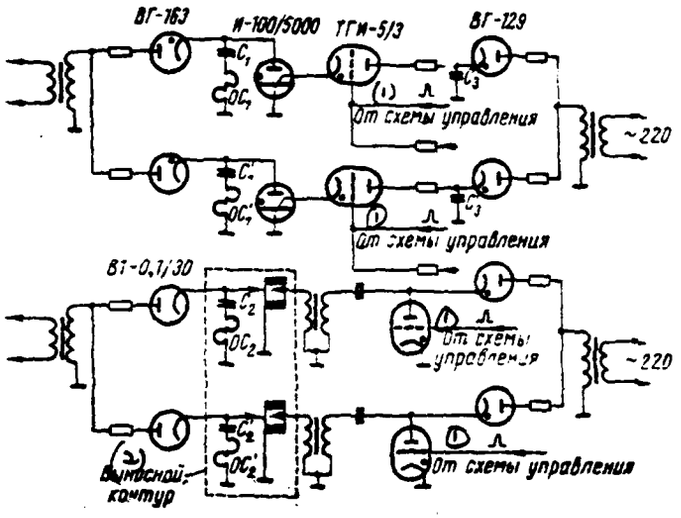

Fig. 7. Schematic diagram of shift and discharge/break of the accelerated electrons tc the target.

Key: (1). Frcm the diagram of ccntrcl. (2). Extensicn contc ur/outline.

Page 46.

Therefore we proposed the combined method of shift, which accomplishes/realizes a discharge/break of the accelerated electrons to the target into two stages. First with the aid of the toroidal winding, or the winding, arranged/lccated on the central insert/bushing, is produced the symmetrical expansion of equilibrium orbit from r_0 to certain r_1, clcse to a radius target location $r_м$.

After this is switched on the second winding of discharge/break, which generates the sharp azimuthal disturbance of magnetic field in orbit of radius r_1, which causes the discharge/break of electrons to the target during several ten turns of electron beam in orbit.

The schematic diagram of the preliminary expansion of orbit is represented in Fig. 7. Preliminary expansion is produced to a radius r_1=32.5 cm, with n=0.9 (it is determined by magnetic measurements). Initial data for calculating the diagram of high-current betatron 25 MeV following:

radius of the equilibrium orbit r_0 ... 24 cm

radius of alignment of target $r_м$ ... 34 cm

gap on a radius δ_0 ... 21 cm

magnetic intensity at the moment of expanding the orbit H_0 ... 3815 oerst.

a radius of central inserts/bushings $r_ц$ ... 13 cm

induction in the center at the moment of expansion $B_ц$ ... $14 \cdot 10^3$ G

the index of drop n in an equilibrium orbit ($r=r_0$) ... 0.5

a radius of pole $r_п$ ... 42 cm

operating cycle impulse circuits T ... 4 s.

For the preliminary expansion it is possible to utilize a sector winding with the scope/coverage of azimuthal round angle.

An increment in the magnetic field ΔH is determined from the formula

$$\Delta H = H_0 \left[\frac{r_0}{r_1} - \left(\frac{r_0}{r_1} \right)^n \right]. \qquad (85)$$

The space, in which is created a supplementary increment in the field, it is determined approximately from the relationship/ratio

$$V = \pi (r_п^2 - r_0^2) \delta_0. \qquad (86)$$

Page 47.

Quadergy $A_м$, reserved in the magnetic field of this space with the intensity/strength ΔH, is equal to

$$A_м = \frac{10^{-8}}{0{,}8\pi} \int_V (\Delta H)^2 dV \approx \frac{10^{-8}}{0{,}8\pi} (\Delta H)^2 V. \qquad (87)$$

The product of the amplitudes of voltage and current in the discharge

circuit is found from the expression

$$I_{макс} U_{макс} = \omega A_м = 2\pi f_0 A_м, \qquad (88)$$

where f_0 - natural vibration frequency in the discharge circuit, it is selected in limits $(5-10) \cdot 10^3$ of Hz, depending on $\tau_и$. Being given amplitude $U_{макс}$, it is possible to determine $I_{макс}$ and a number of turns of the winding of expansion c.

The inductance of bias coil

$$L = 1{,}26 \cdot 10^{-8} \frac{w^2 S}{r_0}, \qquad (89)$$

where $S = \pi(r_н^2 - r_c^2)$ - area of the ring, included by the turns of winding.

Capacity/capacitance in the discharge circuit is found from equation for the energy

$$A_м = \frac{CU_{макс}^2}{2}, \qquad (90)$$

whence

$$C = \frac{2A_м}{U_{макс}^2}. \qquad (91)$$

With known $I_{макс}$, and C of contour/outline it is possible to calculate characteristic impedance $\rho = \sqrt{L/C}$, the strength of effective current $I = I_{макс} \sqrt{\tau/2T}$ and energy factor of contour/outline $Q = \rho \cdot R_{пр}$, and $R_{пр} = \rho l / S_{пр}$ - the resistor/resistance of the wire of the displacing winding. The results of calculation are given in Table 1.

Voltage in the contcur/outline is equal to 5 kV. As the commutating instrument is selected the ignitien rectifier of the type I-100/5000. The calculatien of the system of the final collection of electrons tc the target is produced on the basis of following initial data:

initial radius r_1 ... 32.5 cm

required increase in the radius Δr ... 1.5 cm

intensity/strength of field $H=Hr_0/r_1$ at the moment of discharge/break in orbit with a radius of $r_1=32.5$ cm ... 2700 oerst.

the index of the drcp of field n in orbit with a radius of $r_1=32.5$ cm ... 0.9.

Remaining initial data the same as for calculating the diagram of preliminary expansion.

The final discharge/break cf electrons is accomplished/realized by azimuthal disturbance cf field in the working zone by winding with angle of $\varphi_1=120°$. The amplitude cf the intensity/strength of the

field, created by the winding of the final discharge/break of electrons, must provide not only an increase in the radius of orbit to $r_м$, but also given speed of the motion of orbit, necessary for obtaining emission impulse by the duration not more than $0.2 \cdot 10^{-6}$ s.

Let the intensity/strength ΔH of the exciting magnetic field change according to the sinusoidal law:

$$\Delta H = \Delta H_м \sin \omega t, \qquad (92)$$

where $\Delta H_м$ - amplitude value of the strength of the distorting field; ω - natural vibration frequency in charging circuit.

With azimuthal disturbance of magnetic field an increase of the radius of orbit Δr in the site of installation of target is determined by the expression

$$\Delta r = r_1 \frac{\Delta H_м \sin \omega t}{H} \cdot \frac{1}{1-n} \cdot \frac{\sin\left(\frac{\varphi \sqrt{1-n}}{2}\right)}{\sin\left(\pi \sqrt{1-n}\right)}. \qquad (93)$$

Table 1. Calculated parameters of bias coil.

(1) ΔH_1, эрст	V, см³	(2) $J_м$, а/мм²	$I_{макс}$, а	(3) W, витков	(4) L, гн	(5) $R_{пр}$, ом	Q	(6) C, ф
−500	$1{,}05\cdot10^5$	125	1470	6	$108\cdot10^{-6}$	0,16	20,6	10^{-6}

Key: (1). cerst. (2). J. (3). turns. (4). H. (5). ohm. (6). f.

Page 49.

After substituting into expression (93) of value r, H, n and Φ, we will obtain

$$\Delta r = 4{,}65\cdot10^{-2}\,\Delta H_м \sin\omega t. \qquad (94)$$

The speed of the radial motion of orbit is determined by the derivative of expression (94)

$$v_р = \frac{d(\Delta r)}{dt} = 4{,}65\cdot10^{-2}\,\omega\Delta H_м\cos\omega t. \qquad (95)$$

With assigned Δr and $v_р$ equations (94) and (95) have three unknowns: $\Delta H_м$, ω and t. For the assignment of the third condition we utilize relationships/ratios (87) and (88). After assuming that product $I_м U_м$ must have the minimum value (for facilitating the selection of the commutating instrument), we will obtain

$$U_м I_м = \frac{10^{-7}\,\omega}{4\pi}(\Delta H_м)^2 V, \qquad (96)$$

where V - space, included by the winding of discharge/break. When $\varphi_1 = 120°$, $V = V_п/3$ см³, where $V_п$ - full/total/complete space of gap, moreover $V_п = 1{.}05\cdot10^5$ см³. Then

$$U_м I_м = \frac{10^7}{4\pi}\cdot\frac{V_п}{3}(\Delta H_м)^2\omega = 2{,}8\cdot10^{-4}(\Delta H_м)^2\omega. \qquad (97)$$

Assuming that at the moment of approach with the target the radial size/dimension of electron beam does not exceed d=0.5 cm, we determine the speed of the radial displacement of the orbit:

$$v_p = \frac{d}{\tau},$$

where τ - duration of the pulse of measurement (time of the "incidence/drop" in the bundle on the target).

Let us introduce the designations:

$$\left.\begin{aligned} a &= \frac{\Delta r}{4{,}65\cdot 10^{-2}}; \quad b = \frac{v_p}{4{,}65\cdot 10^{-2}}; \\ c &= \frac{U_M I_M}{2{,}8\cdot 10^{-4}}; \quad x = \Delta H_M \end{aligned}\right\} \qquad (98)$$

Page 50.

Then from relationships/ratios (94), (97) and (98) we obtain:

$$\left.\begin{aligned} x\sin\omega t &= a; \\ x\omega\cos\omega t &= b; \\ x^2\omega &= c. \end{aligned}\right\} \qquad (99)$$

We convert system (99) to the form:

$$\left.\begin{aligned} \sin\omega t &= \frac{a}{x}; \\ \cos\omega t &= \frac{b}{x\omega}; \\ \omega &= \frac{c}{x^2}, \end{aligned}\right\}$$

whence it is easy to obtain biquadratic equation relative to x:

$$x^4 - \frac{c^2}{b^2}x^2 + \frac{a^2c^2}{b^2} = 0. \qquad (100)$$

The solution of equation (100)

$$x^2 = \frac{c^2}{2b^2} \pm \sqrt{\left(\frac{c^2}{2b^2}\right)^2 - \left(\frac{ac}{b}\right)^2}$$

has real roots under the condition

$$\left(\frac{c^2}{2b^2}\right)^2 \geqslant \left(\frac{ac}{b}\right)^2,$$

whence

$$c \geqslant 2ab.$$

If we make $c = 2ab,$

positive decision of equation (100)

$$x = \Delta H_{\text{м}} = \frac{c}{b\sqrt{2}} = \frac{2ab}{b\sqrt{2}} = a\sqrt{2}. \quad (101)$$

Page 51.

From the first and second equations of system (99) taking into account (101) we will obtain

$$\sin \omega t = \cos \omega t = \frac{1}{\sqrt{2}},$$

whence

$$\omega t = \frac{\pi}{4} \quad \text{and} \quad t = \frac{\pi}{4\omega}.$$

Thus, all necessary parameters of system (99) are determined unambiguously.

The fundamental design parameters of the diagram of final discharge/break are determined just as for the preliminary expansion of orbit, (they are given in Table 2).

The given calculation of the diagrams of the expansion of orbit and discharge/break of electrons to the target is approximate, since it does not consider the leakage fluxes of the windings of the expansions and discharge/break, which (flows) have vital importance, especially for the high-current betatrons, which possess the large sizes/dimensions of working zone. Therefore the final values of the parameters of circuits of shift and discharge/break of electrons are corrected and are more precisely formulated experimentally on the accelerator in operation.

In the examination of the process of the discharge/break of electrons to the target in the high-current betatron should be considered emf of the self-induction of the accelerated bundle, which appears during the interruption of the ring current of electrons in the process of its collision with the target. This emf of self-induction on radius r is determined by rate of change in the intensity/strength of field $\dot{H}_z$, caused by the ring current of the beam:

$$\mathscr{E} = -\frac{1}{c} \cdot \frac{\partial}{\partial t} \left(\frac{H_z r}{2} \right). \qquad (102)$$

Table 2. Calculated parameters of the winding of discharge/break.

(1) ΔH, эрст	V, см³	(2) $A_м$, дж	$I_м$, а	(3) W, витков	(4) L, гн	(5) $R_{пр}$, ом	(6) C, ф	(7) $U_м$, в	(8) τ, мксек
45,5	$0,35 \cdot 10^5$	0,29	400	2	$4 \cdot 10^{-6}$	0,85	10^{-7}	$8 \cdot 10^3$	0,188

Key: (1). cerst. (2). J. (3). turns. (4). H. (5). ohm. (6). f. (7). V. (8). μs.

Page 52.

Intensity/strength H_z of the magnetic field of ring current is determined by the relaticnship/ratic

$$H_z = \frac{2\pi I}{cr}. \qquad (103)$$

Then we obtain for $\mathscr{E}$

$$\mathscr{E} = -\frac{1}{c} \cdot \frac{\partial}{\partial t}\left(\frac{2\pi I}{cr} \cdot \frac{r}{2}\right) = -\frac{1}{c} \cdot \frac{\partial}{\partial t} \cdot \frac{2\pi I}{2c} = -\frac{\pi}{c^2} \cdot \frac{\partial I}{\partial t}. \qquad (104)$$

The energy, acquired by electron for one turn, will be

$$\mathscr{E}_{об} = eU_{об} = 2\pi rEe = \frac{2\pi^2 re}{c^2} \cdot \frac{\partial I}{\partial t}. \qquad (105)$$

Speed will be determined by the ratio of the time of beam spill of electrons $t_{сбр}$ to the time of one turn $t_{об}$.

$$N = \frac{t_{сбр}}{t_{об}}. \qquad (106)$$

Then a full/total/complete increase in energy of one electron for the time or the discharge/break

$$\Delta \mathscr{E} = eU_{об}N = \frac{2\pi^2 re}{c^2} \cdot \frac{t_{сбр}}{t_{об}} \cdot \frac{\partial I}{\partial t}. \qquad (107)$$

For the specific case let us accept following data: the time of discharge/break $t_{c6p}=2\cdot10^{-7}$ s (because of the short time of discharge/break the presence of iron, which is found within the circular electron beam, it is possible not to take into consideration). Ring current I let us accept equal to 50 A. Radius of target location $r_м=34$ cm. Then from formula (107) we obtain

$$\Delta\mathscr{E}=\frac{2\cdot3.14^2\cdot34\cdot4,8\cdot10^{-10}}{9\cdot10^{20}}\cdot\frac{2\cdot10^{-7}}{4,9\cdot10^{-9}}\cdot\frac{50}{2\cdot10^{-7}}\cdot3\cdot10^9=$$

$$=3,5\cdot10^{-7}\text{ erg},$$

where $t_{o6}=4.9\cdot10^{-9}$ s, or

$$\Delta\mathscr{E}=3,5\cdot10^{-7}\cdot6,25\cdot10^4=219\text{ keV}.$$

Page 53.

This supplementary energy acquire latter/last beam electrons due to emf of self-induction, which appears upon the decomposition of ring current I=50 and for the time $0.2\cdot10^{-6}$ s.

Consequently, emf of self-induction, causing the supplementary acceleration of the circulating electrons in the process of their discharge/break to the target, leads to an additional increase in the radius of orbit and thereby it contributes to an increase in the

speed of the shift of electrons by the target, i.e., to shortening the duration of emission impulse. The effect of emf of the self-induction of beam is greater, the greater the accelerated ring current I and the less the time of discharge/break $t_{сбр}$.

§9. Operating diagrams of the shift of high-current betatrons.

The schematic diagram of the displacement of a heavy-current betatron of 25 MeV which ensures obtaining a radiation pulse with a duration less than $2 \cdot 10^{-7}$ s is shown in Fig. 7.

The preliminary expansion of orbit is accomplished/realized by winding OC_1 (it encompasses the shaped part of the poles), through which is discharged preliminarily charged/loaded capacitor C_1. Charging C_1 to U= 5 kV is produced by rectifier on the tube VG-163. As the commutating instrument is used the ignition rectifier of the type I-100/5000. The igniting impulse/momentum/pulse is generated by the capacitor discharge C_3, of that charged from the rectifier on the gas-filled tube rectifier VG-129. As the commutating instrument in the circuit of the ignition of ignition rectifier serves thyratron TG1-5/3.

The final discharge/break of electrons to the target is produced with the aid of the sector winding OC_2 with azimuthal angle of 120°. Capacitor C_2 is charged from the rectifier on the tube V1-0.1/30. As the commutating instrument is used the controlled three-electrode) the discharger/gap, which possesses the very small inductance (the hundredths of microhenry). The electrodes of discharger/gap are

prepared from the tungsten. The cathode of discharger/gap is assembled from the tungsten rods with a diameter of 0.6 mm in the form of cylinder with the generatrix of h=12 mm. Control electrode is placed within the cathode and is isolated/insulated from it by porcelain tube. The anode is prepared from the continuous tungsten molding/bar of rectangular cross section and has sizes/dimensions 5x5x10 of mm. The construction/design of fastening the anode and control electrode allows/assumes necessary gap adjustment of discharger/gap. Electrodes are fastened/strengthened in the brass mountings/cases and are encased from the organic glass, which uses for the electrical insulation of electrodes. The operational stability of discharger/gap is $0.1 \cdot 10^{-6}$ s, which completely satisfies the requirements, presented to the jettison system of electrons for the target.

The schematic of the triggering of discharger/gap is analogous to the diagram, used in the circuit of the triggering of the ignition rectifier of the system of preliminary expansion.

For reducing to the minimum of the inductance of the discharge circuit of the winding of discharge/break in it must be a minimum number of turns - two; they are made from aluminum twig and are placed within vacuum chamber above and under median plane of betatron. The parts of discharge circuit are mounted in the form of

the separate block, adjusted in immediate proximity of the accelerator. Storage capacity/capacitance is comprised their three parallel-connected non-inductive capacitors of the type IM100-0.1 with the total capacitance of 0.3 μF.

Because of the enumerated measures the inductance of the discharge circuit of the diagram of final discharge/break is entire $5 \cdot 10^{-8}$ H. The diagram of preliminary expansion and the charge part of the diagram of final discharge/break are mounted in the separate cabiret, both parts of the system of shift, shown in Fig. 7, have two parallel channels, since pulse betatron was made in the form of the two-chamber construction/design, which has two independently working accelerative systems.

As a result of understable work of ignition rectifiers I-100/1000 in the mode/conditions of narrow pulses the ignition rectifiers are replaced by thyratrons of the type TR-85/15. The measurements of the distribution of the magnetic field of the windings of discharge/break showed that the maximum of the strength of field falls to the region of the equilibrium radius r_0, if winding encompasses radial size/dimension $r_в - r_c$. Therefore in the final version an inside radius of the winding of discharge/break $r_в$ is more than radius r_0.

The made system of the shift of the orbit of electrons ensured obtaining the amplitude of current to 2000 A with the duration of 350 μs with the voltage of 5000 V in the diagram preliminary expansions of orbit and current pulse in amplitude to 1400 A, with duration of $8 \cdot 10^{-6}$ s with the voltage of 8000 V in the reset circuit of electrons on the target.

With the aid of this system is obtained the impulse/momentum/pulse of bremsstrahlung with the maximum energy 25 MeV for the duration less $0.2 \cdot 10^{-6}$ s. The oscillogram of emission impulse, taken with the aid of the photomultiplier with the diagram on the cathode follower, is represented in Fig. 8. During the upper scanning/sweep of oscillogram is fixed the reference pulse by duration $0.2 \cdot 10^{-6}$ s, during the lower scanning/sweep - emission impulse.

The schematic diagram of the shift of electrons from the equilibrium orbit in the high-current betatrons, which work at the frequency of 50 Hz, is analogous described above. Difference lies in the fact that for decreasing the power of rectifying device/equipment in the discharge circuit of the diagram of expansion is established/installed one additional recharging valve/gate, and in the reset circuit instead of the discharger/gap are applied hydrogen thyratron of the type TGI. The replacement of dischargers/gaps by

thyratrons is caused by the limited service life of the dischargers/gaps, which maintain/withstand abcut 100000 imp, which with the work with the frequency cf 50 Hz comprises less than one hcur.

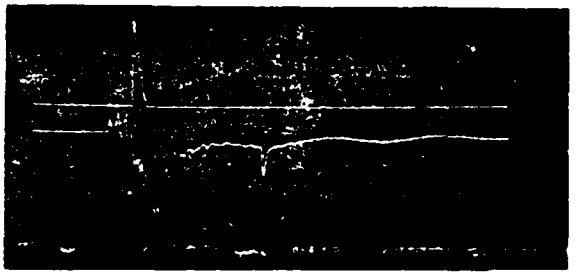

Fig. 8. Oscillogram of emission impulse.

Page 56.

If obtaining short emission impulse is nct required, the discharge/break of electrcns tc the target is accomplished/realized by a diagram of the expansion cf crbit. In the discharge device/equipment and the discharge circuit for this it is necessary to have only certain reserve according to the power. In this case the duration of emission impulse is obtained in limits $(4-10)\cdot10^{-6}$ s.

Chapter 4.

SOME CHARACTERISTICS OF BEAM AND RESULTS OF THE LABORATORY TESTS OF HIGH-CURRENT BETATRON.

§10. Measurement of the charge of the beam, accelerated in the betatron.

The measurement of charge Q of the beam, accelerated in the betatron, is fairly complicated task, since there does not exist the direct method of measuring this value. By this is explained the existence of a large number of different methods, with the aid of which are made the measurements of the introduced, seized and circulating in the betatron current.

To measure the charge of the beam, introduced in the acceleration, is possible by many methods, for example, by the method of magnetic belt/zone, by the method of turns on the central core, etc. The same methods can be utilized, also, for measuring the charge of beam at the end of the cycle of acceleration. However, the measurements of the charge of the discarded beam hinder by those

operating at the moment of the shift of the accelerated electrons from the equilibrium orbit by powerful/thick electromagnetic fields, caused by the work of the pulse current generator of the diagram of shift, interferences from which considerably exceed useful signal. The screening of measuring devices in the betatron is almost impossible, since introduction into the working gap of ferromagnetic or massive nonferromagnetic shield distorts the controlling magnetic field of betatron, leading at best to a sharp decrease in the number of trapped into acceleration electrons. It is necessary to consider also that the charge, led to the end/lead of the cycle of acceleration, is substantially less than the charge of beam, trapped into acceleration, which respectively decreases the value of the useful measured signal.

For measuring the magnitude of the charge of beam, discarded to the target at the end of the cycle of acceleration, it is possible to utilize the procedure, used on the betatron 15 MeV. Method consists in the measurement of electronic current directly from the target in small phases of the discharge/break of the electrons from the orbit, which correspond to energy on the order of 1 MeV. With the energies of electron, which exceed 10-12 MeV, the current from the target considerably differs from true current, since the path/range of electron in the material of target (tungsten) is 4-5 mm, whereas the real thickness of target does not usually exceed 1 mm. Therefore the

large part of the accelerated electrons threads target right through and, therefore, is not recorded by measuring meter. It is more than that, under the action of the electron bombardment of target from its material are freed/released secondary, tertiary and so forth the electrons. If the part of these electrons leaves target, instrument will record a decrease in the current from the target. When the emission of secondary electrons is sufficiently great, instrument shows the current whose polarity is opposite expected. For determining the true number of electrons, which experienced collision with the target, it is necessary to consider the electrons, reflected by the material of target. The reflection of electrons with the energy from several ten kilcelectronvolts to 1.75 MeV for the materials of target over a wide range z is in detail investigated by Seliger and recently by Dressel [10]. The coefficient of reflection of electrons is defined as the ratio of a difference in total number of electrons, recorded by counter, and an initial number of electrons to an initial number of electrons, i.e.

$$\beta = \frac{n_{пол} - n_{нач}}{n_{нач}} = \frac{n_{пол}}{n_{нач}} - 1, \qquad (108)$$

where $n_{нач}$ - number of electrons, recorded by instrument in the absence of the reflecting sample/specimen (in our case - target); $n_{пол} = n_{нач} + n_{отр}$ - number of particles, recorded by the same instrument at the same point taking into account the electrons reflected, i.e., in the presence of the reflecting sample/specimen (target); $n_{отр}$ - number of the electrons reflected.

For Z=74 (tungsten) and the range of energies of electron to 1.7 MeV coefficient β=0.8.

In the expression for determining the magnitude of the charge of beam, jettisoned to the target soon after the termination of injection, it is necessary to introduce correction for reflection in the form of term $(1-\beta)^{-1}$. Then, assuming that the current pulse from the target has sinusoidal form, the charge of the discarded beam can be calculated according to the formula

$$Q_м = \frac{I_м t}{1{,}57R}(1-\beta)^{-1} \qquad (109)$$

where $I_м$ - amplitude value of current pulse from the target; t - duration of current pulse and β=0.8 - coefficient of reflection of electrons by tungsten target. Product in the right side of the formula is numerically equal to the area of current pulse from the target. Value $I_м$ will be determined from expression $I_м = U_м/R$, where $U_м$ - amplitude value of a voltage drop across resistor/resistance of R, through which leaks off the measured current of the fallen to the target electrons. Then equation (109) takes the form

$$Q_м = \frac{U_м t}{1{,}57R}(1-\beta)^{-1}. \qquad (110)$$

Signal amplitude from the target is greatest in small phases of shift, i.e., with the kinetic energy of electrons 0.4-1 MeV. The amplitude of this signal on the resistor/resistance of 100 ohms

composes 1.5-3.5 V. With an increase in the phase of shift occurs the decrease of signal amplitude from the target and, in the phase of approximately 1800 μs, which corresponds to energy of electrons 7-8 MeV, is planned tendency toward a change in the polarity of pulse (Fig. 9). A larger increase in the phase leads to a change in the signal polarity whose amplitude virtually does not depend on further increase in the energy of electrons.

The voltage pulse from the target of high-current betatron to 25 MeV, created by the current of electrons on the resistor/resistance of 100 ohms with ϕ=100 μs after the termination of injection (E=0.7-0.8 MeV, has an amplitude, equal to 3.5 V for the duration 3 μs. The electronic charge, calculated according to formula (104), it is equal to

$$Q_{\text{м}} = \frac{U_{\text{м}} t}{1{,}57R}(1-3)^{-1} \approx 8{,}9\cdot 10^{-7}\text{ к}. \qquad (111)$$

which corresponds to a number of accelerated electrons $N=Q/e=5.56\cdot 10^{12}$. This quantity of electrons in the high-current betatron 10^3 times of more than the appropriate value, attained in the majority of the best samples/specimens of usual betatrons in which charge does not exceed $5\cdot 10^5$ electro-neutrons/pulse.

Page 60.

There is greatest interest in the measurement of the electronic

AD-A098 407 FOREIGN TECHNOLOGY DIV WRIGHT-PATTERSON AFB OH F/G 20/7
HIGH-CURRENT BETATRON AND STEREOBETATRON.(U)
FEB 81 A A BOROBYEV, V A MOSKALEV
UNCLASSIFIED FTD-ID(RS)T-1715-80 NL

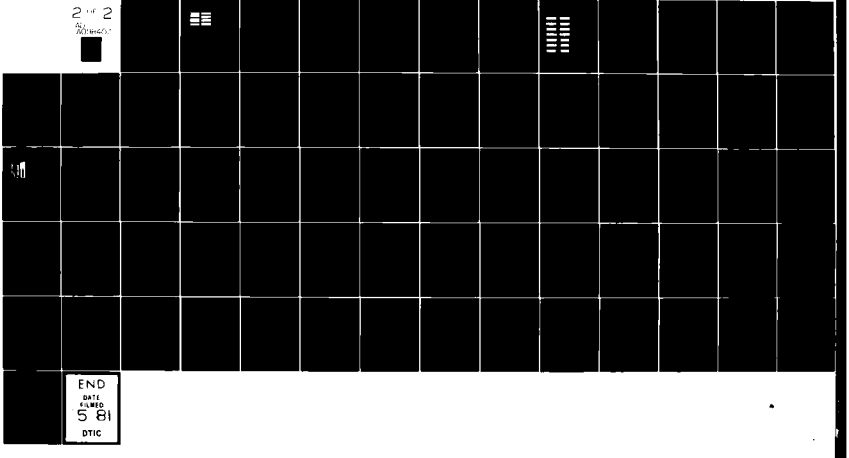

END
DATE FILMED
5 81
DTIC

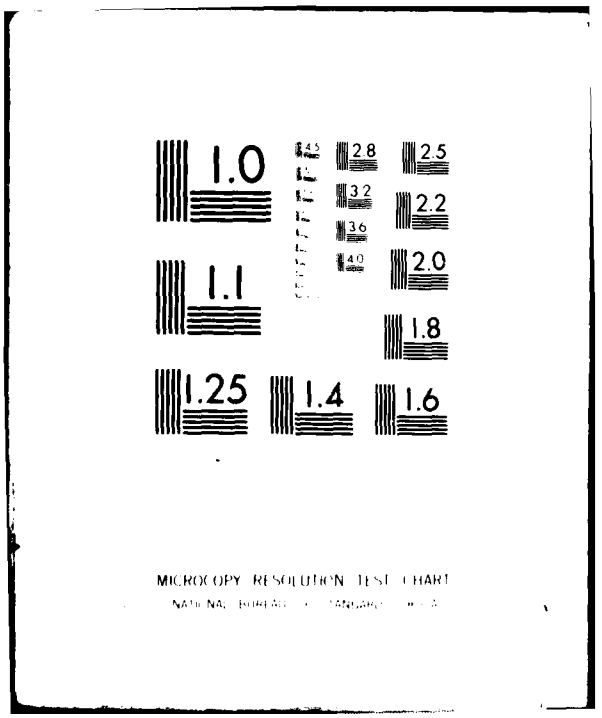
1.0
1.1
1.25
1.4
1.6
1.8
2.0
2.2
2.5
2.8
3.2
3.6
4.0
MICROCOPY RESOLUTION TEST CHART

charge of beam, led in the betatron to the end/lead of the cycle of acceleration. The method of recording the current from the target does not give the possibility to fulfill these measurements on reasons indicated above. However, the current pulse, removed from the target with small ϕ (i.e., with small E), can be used for the calibration of any other sensor, for example signal electrode.

As the signal electrode-indicator were used two sector turns with the azimuthal angle in 120°, made from aluminum wire and placed within vacuum accelerative chamber at a distance of $r>r_0$. Turns were arranged/located above and under median plane of betatron and in the usual mode/conditions of work of the accelerator were utilized as the displacing winding for obtaining the short emission impulse.

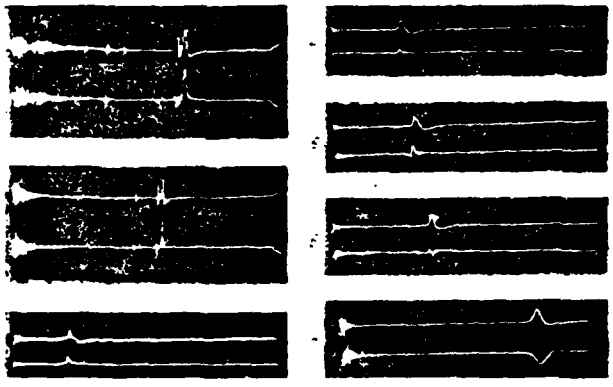

Fig. 9. The oscillograms of current pulse from the target and from electrode-indicator: in all photographs upper oscillogram shows the voltage pulse from electrode-indicator R=91 ohm, lower - voltage pulse from the target. In the expasion stage of the orbit of the beam of equal to 1) ϕ=180 μs; 2) ϕ=400 μs; 3) ϕ=1020 μs; 4) ϕ=1260 μs; 5) ϕ=1500 μs; 6) ϕ=1800 μs; 7) ϕ=3060 μs.

Page 61.

The connection/communication of signal from the target and the signal from electrode-indicator with the different energies of the accelerated electrons E is illustrated by Fig. 9. Before the impulses/momenta/pulses being investigated is visible the random noise from the impulse circuit of auxiliary designation/purpose. The impulse/momentum/pulse of the lower oscillogram Fig. 9 corresponds to energy of electrons of approximately 20.5 MeV (ϕ=3060 μs). In the

duration of pulse 11.5 μs, the amplitude of voltage 120 mV (R=91 ohm) the impulse/momentum/pulse corresponds to a charge $4.7 \cdot 10^{-7}$ k, or a number of electrons in the impulse/momentum/pulse of order $3 \cdot 10^{12}$. This value 600 times exceeds a number of particles, accelerated in usual betatrons ($\sim 5 \cdot 10^{9}$).

Thus, at the beginning of the cycle of acceleration in the chamber/camera of high-current betatron circulates the electronic charge, equal to $8.9 \cdot 10^{-7}$ k. It creates circulating in orbit electronic current, equal to

$$I_{\text{u. нач}} = Q \frac{\beta c}{2\pi r_0} = 167 \text{ a}. \qquad (112)$$

where Q - charge; $\beta = v/c$ - relative velocity of electrons; $c = 3 \cdot 10^{10}$ cm/s - speed of light. At the end of the cycle of acceleration the electronic charge, equal to $4.7 \cdot 10^{-7}$ k, creates the circulating in orbit current, equal to

$$I_{\text{u. кон}} = Q \frac{c}{2\pi r_0} = 4{,}7 \cdot 10^{-7} \frac{3 \cdot 10^{10}}{150} = 94 \text{ a}. \qquad (113)$$

Then avarage/mean in the cycle of acceleration circulating in orbit current is 130 A. The accelerated beam in the high-current betatron is dumped to the target for the time of 0.1-0.2 μs. The pulse current of electrons to the target with the charge $4.7 \cdot 10^{-7}$ to the duration of emission impulse $\tau_и = 0.2$ μs, comprises

$$I_и = \frac{Q}{\tau_и} = 2{,}35 \text{ a}, \qquad (114)$$

but with $\tau_и = 0.1$ μs $I_и = 4.7$ A.

It is necessary to note that the corrected numerical values are obtained on the basis of the measurements, carried out with one of the usual operating modes on the accelerator. In a number of cases the charge of the beam, trapped into acceleration, exceeds the corrected here values.

§11. Investigation of beam in the process of acceleration the lateral instability of beam in the betatron.

During the experimental investigation of the process of accelerating the beam of electrons in the first high-current betatron in 1960 was discovered the phenomenon of the lateral instability of the circulating electron beam. Instability appears in the shaped beam after the considerable time after the end of the process of injection and is evinced by the periodic increase of the amplitude of the bouncing of electrons for a radius of equilibrium orbit to the vertical size/dimension of accelerative chamber/camera for $r=r_0$. For a certain period of time (from 15 μs more) beam "scratches" chamber walls, losing on them the part of its electrons. Then the amplitude

of betatron oscillations is decreased, becoming less than the vertical size/dimension of chamber/camera. After certain time (on the order of hundred or hundreds of microseconds) the process again is repeated, being accompanied every time by the death of the part of the accelerated electrons on the chamber walls. In entire cycle of acceleration can be lost 60-90% of the seized into the acceleration number of electrons. In this case on the aquadag of chamber/camera remains clear beam trace in the form of dark/nonluminous circular paths/tracks with the radial size/dimension approximately 10 mm and the well-marked boundaries. Paths/tracks are arranged/located on the upper and lower chamber walls accurately on radius r_0 of the equilibrium orbit of electrons.

With the aid of the procedure, described in the preceding/previous paragraph, for the high-current betatron on 25 MeV are obtained the oscillograms of the impulses/momenta/pulses of the spontaneous discharge/break of electrons to the chamber walls (see Fig. 10). The picture, represented in Fig. 10, to a considerable extent depends on the conditions of injecting the electrons in the betatron, i.e., from a number of trapped into acceleration particles. Changing the conditions of injection, it is possible to obtain from 1 to 8-9 impulses/momenta/pulses or one reset pulse.

It is characteristic that independent of a number of reset pulses, which occur in the process of accelerating the beam, the rate of the dose of the bremsstrahlung of betatron remains in effect constant, and to the end/lead of the cycle of acceleration always "lives" an approximately identical number of electrons.

The full/total/complete time, during which is observed the phenomenon of the lateral instability of beam, in our experiments 1500-1600 μs, which corresponds to an compcsas energy of the accelerated electrons of approximately 10 MeV.

It was at first assumed, that the instability of beam is caused by resonance phenomena, caused by the fact that the value of the coefficient of the drop of magnetic field n in the betatron was equal to 0.5 on radius r_0. In connection with this the pole of betatron they were replaced new (see Fig. 3). Value n in the latter case was equal to 0.6 and was retained approximately constant on a radius. However, the picture of the instability of electron beam remained previous. The late onset of the instability of beam in the transverse direction experimentally was observed in the resonance particle accelerators and in the accumulators/storage.

The appearing recently investigations of the coherent instability of beam in the accelerators and the accumulators/storage shed light on the nature of this phenomenon. In work [15] is theoretically investigated transverse electromagnetic interaction of intense, uniform in the azimuth beam with itself taking into account the effect of the resistor/resistance of the walls of vacuum chamber.

The beam of particles, which rotates with the angular frequency ω_0 and which accomplishes coherent bouncing, generates travelling waves whose angular frequency is equal to $\omega=(1+\nu)\ \omega_0$, where ν - number of betatron oscillations per revolution. In the case of the absence of the resistor/resistance of chamber walls these oscillations are stable. In this case on the beam operate the electromagnetic forces, out of phase on 90° with respect to the oscillations of vertical speed of beam and which only a little displace frequency of betatron. If this shift it is sufficient for changing the wavelength of betatron oscillations to the value, which corresponds to any resonance of accelerator, then beam becomes unstable. For this is usually sufficient to change ν to 1/4. Maximum charge for the majority of installations proved to be sufficiently to large ones.

Page 64.

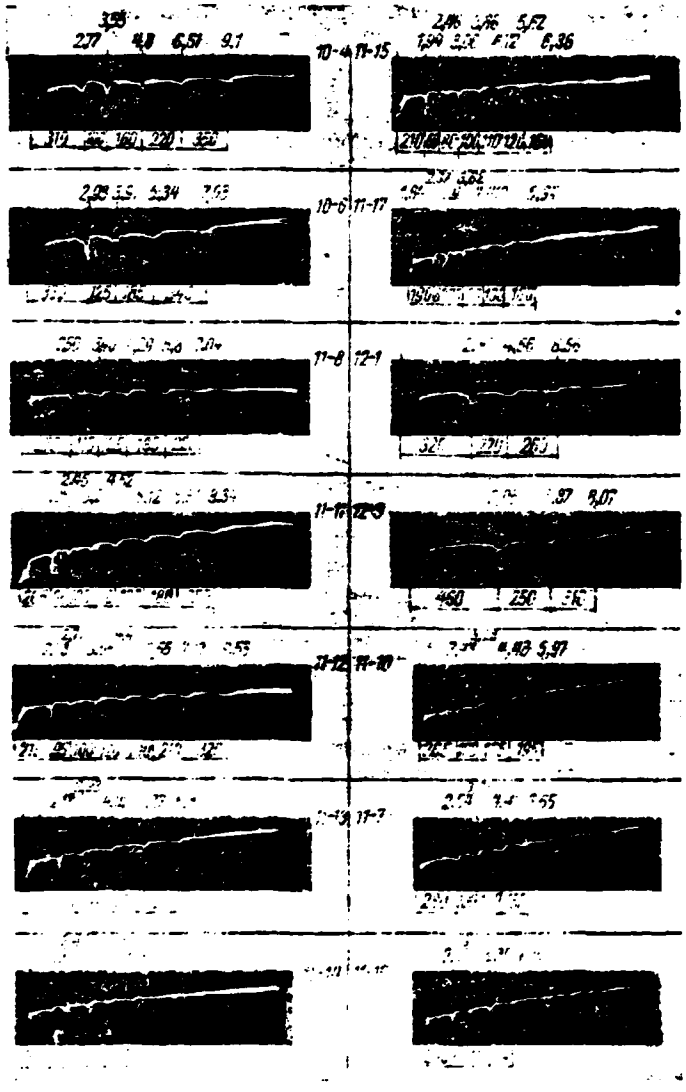

Fig. 10. Oscillograms of reset pulses of electrons in process of accelerations, obtained under varied conditions of injection: numerals under oscillograms show duration of intervals between

impulses/momenta/pulses of "discharge/break", μs; numerals above oscillograms - energy of electrons at moment of "discharge/break", MeV; numerals between oscillograms - series number of experiment.

Page 65.

If the resistor/resistance of walls has finite value, then the fields, caused by wave with the frequency $\omega=(1-\nu)\omega_0$, create the acting on the beam forces with the component, cophasal with the vertical coherent rate. Specifically, this wave can lead to an exponential increase in the transverse oscillations of beam. The energy of transverse motion is taken from the longitudinal particle motion. The electromagnetic forces, connected with the wave by frequency $\omega=(1+\nu)\omega_0$, contain the component, shifted on 180° relative to vertical coherent rate, and they lead to exponential damping of bouncing. In work [15] it is shown that in the case of the beam, which consists of the particles with identical values ν and ω_0, the final conductivity of chamber walls always leads to instability. The time constant of the build-up/growth of instability for the case of betatron is given by the equation

$$\tau_0=\frac{3}{2}\cdot\frac{m_0c^2}{e^2}\cdot\frac{T\nu_z}{\pi N\beta}\cdot\frac{h^2}{c^2}\sqrt{8\pi\sigma(1-\nu_z)\omega_0}, \quad (115)$$

where m_0 and e - mass and electron charge respectively; $\gamma=mc^2/m_0c^2$ - energy of electron in the energy units of rest; $\beta=v/c$ - relative particle speed; c - speed of light in the vacuum; h - vertical

size/dimension of accelerative chamber/camera; $\omega_0=c/2\pi r_0$ - frequency of revolution of particle on the orbit; r_0 - radius of equilibrium orbit; $\nu_z=\sqrt{n}$ - the number of vertical betatron oscillations per revolution; n - index of the drop of magnetic field on a radius; σ - conductivity of the material of coating the walls of accelerative chamber/camera. From the equation it follows that the rate of growth in the instability is proportional to the number of particles in beam N and is inversely proportional $\sqrt{\sigma}$.

Page 66.

For a high-current betatron on 25 MeV the entering equation (115) values have values; $\nu_z=\sqrt{n}=\sqrt{0,6}$, where $\omega_0=c/2\pi r_0$; $r_0=24$ cm; $\sigma=6.3\cdot10^{16}$ Ω^{-1}. The substitution of these values with $N=10^{12}$ in equation (115) gives time constant $\tau_0\approx0.5\cdot10^{-3}$ s, which by an order is less than the duration of the acceleration of electrons in betatron ($t_{уск}=5\cdot10^{-3}$ s). This means that the instability of beam can be developed several times during one cycle of acceleration. Since τ_0 is reduced proportional to decrease γ, then with smaller γ at the beginning of the cycle of acceleration τ_0 will be still less.

From the given in Fig. 10 oscillograms it follows that the developing instability leads to the death only of the part of circulating electronic current in each cycle "automatic reaper". The

decrease of the circulating current leads to the increase of the time, necessary for the develcpment of the subsequent instability, which is accompanied by the next loss of the part of accelerated electronic current. This periodic process continues to those pores, the charge of the circulating current will not be lowered to certain critical value, with which τ_0 becomes more than time t, which remains to the end/lead of the cycle of acceleration, and losses no longer it is observed. Consequently, total electron charge, which remain in orbit after the cessation of "self-ejections", is certain critical maximum charge of the beam which can be "brought" in the high-current betatron to the end/lead of the acceleration. Introduction to chamber/camera and capture in the acceleration of the electron beam the magnitude of the charge of which is more than this critical value, does not lead to an increase in the charge of the accelerated beam, since this "excess" part of the charge perishes on the chamber walls as a result of the developing instability of beam in the vertical direction.

The value of the electronic charge of beam, which circulates in orbit at the different moments of the cycle of acceleration, can be evaluated as follows. Time constant τ_0 is equal to the time, during which the amplitude of the bouncing of beam (i.e., the vertical size/dimension of the accelerated beam) grows/rises in e of times.

Consequently, the vertical size/dimension of beam A grows/rises according to the law

$$A = A_0 e^{t/\tau_0}, \qquad (116)$$

hence

$$\tau_0 = \frac{t}{\ln A - \ln A_0}, \qquad (117)$$

where A_0 - initial size/dimension of beam, A - maximum vertical size of beam, limited to the vertical size/dimension of h of accelerative chamber/camera (in our case of h=16.5 cm) on a radius of equilibrium orbit r_0=24 cm; t - time, necessary for an increase in the amplitude from A_0 to A. It is obvious that in the gap/interval between two beam bursts first is pressed in the vertical direction to certain value of A_0, and then again is expanded to size/dimension of A. Therefore interval t_i between two impulses/momenta/pulses can be developed on two parts, proportional to relation t_{i-1}/t_i. In this case the first part of the interval corresponds to the compression of beam, and the second - to expansion.

Time t, entering expression (117), is determined from the intermediate graphs which can be constructed on the basis of data of the oscillograms (see Fig. 10) taking into account corrections for the increase in the energy of beam in the process of acceleration, and it is written/recorded in the form

$$t = t_i - \frac{t_i t_{i-1}}{t_i + t_{i-1}}. \qquad (118)$$

For determining the initial size/dimension of A_0 of beam, i.e., the size/dimension, to which the beam will be compressed for time t, we will use the equation of the charge density, obtained by P. A. Cherdantsev,

$$\ddot{\eta} + \Omega^2 (e^{\eta} - 1) - F = 0, \qquad (119)$$

where

$$\eta = \ln \frac{\rho}{\rho_0}; \quad \Omega^2 = \frac{4\pi e^2}{m} (1 - \beta^2) \rho_0; \quad F = \dot{\eta}^2.$$

Value of ρ_0 is calculated from formula (16), and F is found from the equation

$$\frac{dF}{d\eta} - F = -\Omega^2 (e^{\eta} - 1). \qquad (120)$$

Page 68.

The solution of the equation of density (119) for plane beam on the assumption that in the beam changes only vertical size/dimension with the constant/invariable width of beam in the radial direction, takes the form:

$$\dot{\eta} = \Omega \sqrt{e^{2(\eta - \eta_0)} - 1 - 2 (e^{2\eta - \eta_0} - e^{\eta})} = \Phi(\eta), (121)$$

where $\eta_0 = \eta$ $(t=0)$. With t=0 the beam has the maximum vertical size of A=h and $\dot{\eta}=0$; in this case $\eta_0=\eta$ and the right side in equation (121) is turned into zero.

From equation (121) it is possible to determine function $t(\eta)$:

$$\frac{dt}{d\eta} = \frac{1}{\dot{\eta}} = \frac{1}{\Phi(\eta)}, \qquad (122)$$

whence

$$dt = \frac{d\eta}{\Phi(\eta)}. \qquad (123)$$

After the integration of expression 8123) in the limits from η_0 and η we will obtain

$$t = \int_{\eta_0}^{\eta} \frac{d\eta}{\Phi(\eta)} = \int_{\eta_0}^{\eta} \frac{d\eta}{\Omega [e^{2(\eta-\eta_0)} - 1 - 2(e^{2\eta-\eta_0} - e^{\eta})]^{1/2}}. \qquad (124)$$

In general this integral is not taken; therefore its value is located by numerical integration.

Determining t acccrding to expression (118) from the oscillogram, it is possible tc find from the graphs the vertical size/dimension of beam A_{oi}, which ccrresponds to time t. It should be noted that value A_0 proves to be approximately identical for all values of energy E of launching/starting, i.e., for any interval t_i. Substituting A_{oi} into expression (117), we find value τ_{oi} for the appropriate i moment/torque of the cycle of acceleration. Substituting τ_{oi} in equatien (115), we obtain numbers of particles N, which circulate in orbit in any time interval between the i-th and (i+1)-th reset pulses of electrons. The results of calculatien for the oscillogram (see Fig. 10, series 11-11) are given in Table 3.

The drop of the current of the charged/loaded particles in the process of acceleration is given on the graph of Fig. 11. Point 3 (see Table 3) for the oscillogram in question falls out from the general/common/total shape of the curve. Remaining six points are placed to the curve. As can be seen from graphs, the loss of electrons as a result of the lateral instability of beam concludes for the data of the cases with the energy of electrons of approximately 10 MeV, decreasing the charge of the seized into the acceleration beam 5-6 times.

Table 3.

(1) Номер точки	(2) Участок осциллограммы	(3) Интервал i, мксек	(4) Энергия в момент t_i, Мэв	(5) N, 10^{12} электронов
1	t_1—0	205	19,6	8,0
2	t_2—t_1	65	2,46	4,4
3	t_3—t_2	100	3,26	3,4
4	t_4—t_3	110	4,52	2,7
5	t_5—t_4	130	5,12	3,2
6	t_6—t_5	180	6,61	2,35
7	t_7—t_6	250	8,34	2,03

Key: (1). Number of point. (2). Section of oscillogram. (3). Interval i, μs. (4). Energy into moment/torque t_i, MeV. (5). N, 10^{12} electrons.

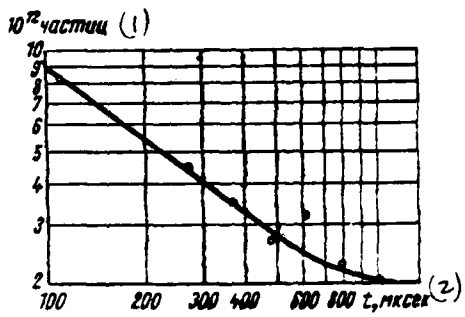

Fig. 11. Decrease of accelerated electron charge due to lateral instability of beam.

Key: (1). particles. (2). μs.

The subsequent slow and insignificant decrease of the charge of beam is caused by the usual reasons (loss on the atoms of residual gas, etc.). Up to the moment/torque of the end of the process of the vertical oscillation of beam a number of particles comprises $2.03 \cdot 10^{12}$ (see Fig. 11). The measured number of accelerated electrons comprises $3 \cdot 10^{12}$, which will agree well with the results of the given above calculations.

Using data of these calculations, it is possible to present qualitatively the picture of the behavior of beam in the high-current betatron in the process of acceleration. This picture is represented in Fig. 12. It is necessary to note that scanning/sweep of oscillograph OK-17M, on which were removed/taken oscillograms, was nonlinear. On the graph of Fig. 12 is represented the oscillogram on the graphic scale of time.

From the figure it is evident that with an increase E and decrease N increases time t, necessary for the oscillation of beam from $A_0 < h$ to $A = h$, where h - vertical size/dimension of chamber/camera on radius r_0.

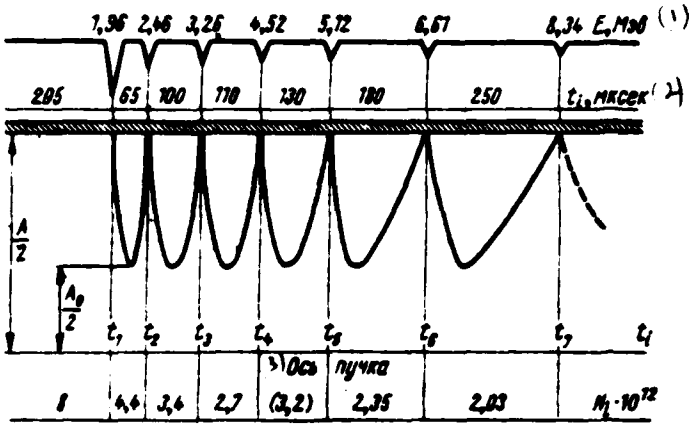

Fig. 12. The qualitative picture of the behavior of beam in the high-current betatron on the graphic scale of time (series 11-11): $A/2$ - half size/dimension of doughnut in z-direction; $A_0/2$ - half size/dimension of beam at the moment of compression.

Key: (1). MeV. (2). μs. (3). Axis/axle of bundle.

Page 71.

After a decrease in the number of circulating electrons to the value of order $(2-3) \cdot 10^{12}$ the time of the development of instability becomes more than the time, which remains to the end/lead of the cycle of acceleration, and this entire beam being retained to the end/lead, it is dumped to the target of accelerator. Thus, for the first time during the creation of betatrons in the high-current

betatrons of TPI they will achieve the limiting current of electrons, the component to $(2-3)\cdot10^{12}$ particles/pulse which can be accelerated in the prescribed/assigned parameters of the magnetic field of accelerator. Limiting current is limited to the onset of the lateral instability of beam, caused by interaction of beam with the conducting layer of coating chamber walls. An increase in the number of seized into the particle acceleration does not lead therefore to an increase in the number of particles, led to the end/lead of the cycle of acceleration, and therefore does not increase the rate of the dose of bremsstrahlung.

§12. Determining the dimensions of focal spot to the target of betatron and the results of the tests of betatrons.

For applying the betatrons in the industrial radiography it is necessary to know the dimensions of the "focal spot", formed by the beam of the accelerated electrons at the end of operating cycle on the target of accelerator. For measuring the sizes/dimensions of focal spot was used the special chamber/camera whose diagram was given in Fig. 13. The beam of the bremsstrahlung of direction into the lead objective, which has the opening/aperture with a diameter of 0.1 mm, and on the photographic film is obtained the inverted image of radiation source, i.e., focal spot on the target of betatron. Objective and chamber/camera are reliably shielded from secondary

radiation by lead shields. The sizes/dimensions of objective and chamber/camera are clear from the drawing. In the test whose diagram is shown for Fig. 13, the image of focal spot on the photographic film was obtained to scale 1:2. Spot has elongated in the vertical direction form with the sizes/dimensions about 1x3 and 0.1x3 mm for the betatrons to 25 and 15 MeV. The obtained sizes/dimensions of focal spot are satisfactory for conducting the majority of practical works and investigations before the flaw detection.

The practical possibilities of pulse betatron during its use for the radioscopy of material in the pulse radiography were evaluated according to the radioscopy of the maximum thickness of lead block.

Page 72.

On the path of the bundle of bremsstrahlung it was placed the lead key, carried out in the form of cube with the side 50 mm, which has on the face, turned to the photographic film, the cylindrical openings/apertures of different depth. Cassette with the film was arranged/located directly after the key and was from behind shielded by the layer of lead. The overall thickness of the absorber before the film changed with supplementary lead blocks. The task consisted of the determination of maximum thickness of the x-rayed material, i.e., this thickness, which "was available" to beam under the most

favorable conditions of radioscopy (fluorescing intensifying screens, most sensitive photographic materials, etc.). As the radiation detector was utilized the x-ray film of firm "Ilford" with fluorescent intensifying screens (front/leading and rear). By one emission impulse it was possible to X-ray the layer of lead with a thickness of 140 mm. In this case on the film was distinguished the image of the openings/apertures of the key, on which was determined maximum x-rayed thickness. Average density of blackening of film 0.7-0.9. The photometric measurement of films was not produced.

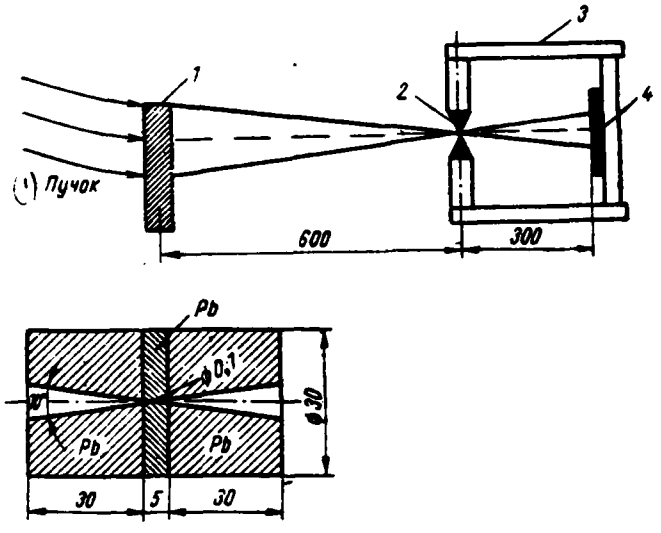

Fig. 13. The diagram of chamber/camera for photographing of the focal spot of betatron: 1 - target; 2 - objective; 3 - chamber casing; 4 - photographic film. Below - the schematic of the construction/design of objective.

Key: (1). Beam.

Page 73.

For the radioscopy of the same block of lead on the betatron of TPI on 30 MeV at the rate of the dose of 70-80 r/min was required the time from three to five seconds, i.e., from 150 to 250 emission impulses. This means that the average/mean radiation dose rate of

high-current betatron per cycle of acceleration is approximately 5 r/cycle, i.e., it is approximately/exemplarily 200 times more than in usual betatron on 30 MeV.

For the laboratory evaluation/estimate of the technical possibilities of high-current betatrons to 25 and 15 MeV, working at the frequency 50 Hz, were carried out some investigations on the radiographic flaw detection of the thick layers of different materials (lead, steel and plastic). In the process of the radioscopy of samples/specimens to the film of type RM-1 and RT-1 were selected the optimum thicknesses of metal intensifying screens on the maximum blackening of film at the minimum for each specific case exposure. Investigated also a change in the necessary thickness of intensifying screen with an increase in the thickness of the x-rayed layer of material. As a result of the filtration of radiation/emission the thickness of front/leading intersifying screen respectively grows/rises. The high intensity of the bremsstrahlung of high-current betatrons makes it possible to considerably reduce the time of exposure with the radioscopy of materials in thickness to 300-400 mm they began to increase both the maximum thickness of the x-rayed material and productivity of the betatron method of control/checking.

Thus, the layer of steel in thickness 200 and 400 mm is x-rayed with the radiant energy 11 MeV and focal length of 1 m for 1.5 and 40

min respectively. But with the energy of emission of 25 MeV and the focal length of 2 m the layer of steel in thickness 200 and 500 mm is x-rayed respectively in 2-3 s and 40 min.

The photographic density of film in all cases was led to 1.6-1.7 units of optical density. Fig. 14a depicts the dependence of the time of the exposure of the radioscopy of different material with the radiant energy 11 MeV on the thickness of absorber. The high intensity of radiation/emission decreases the ill effect of the associated transient processes. Therefore is possible obtaining the detectability of defects in limits of 0.9-1o/o of thickness of the x-rayed layer in entire range of the thicknesses of material (from 200 to 510 mm on steel).

Page 74.

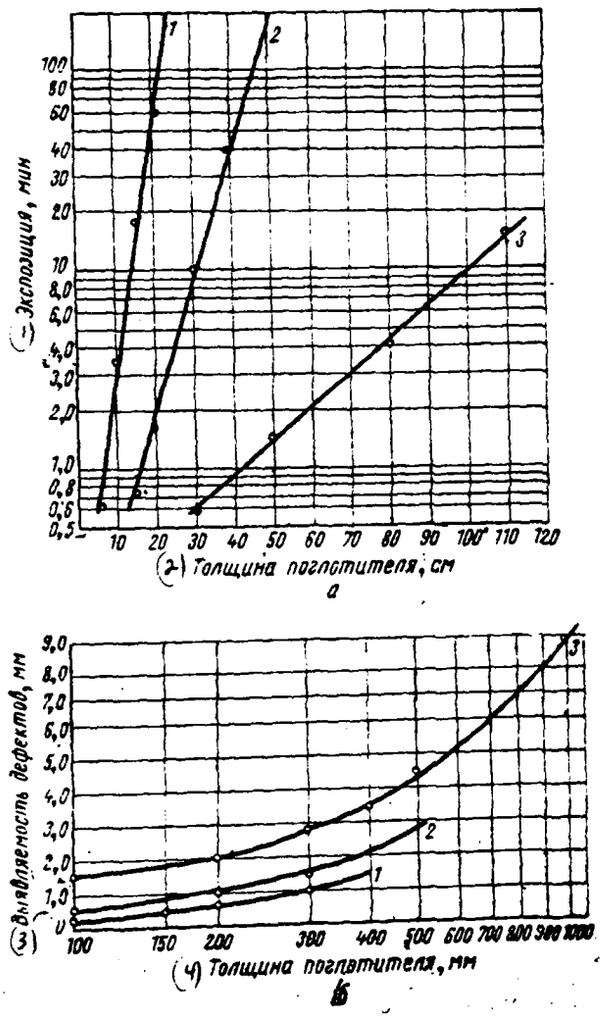

Fig. 14. Graphs of exposures (a) and detectability of defects (b) for case of high-current betatron with energy 11 MeV: 1 - lead, focal length of 1 m, film RM-1, shields 1P2; 2 - steel, focal length of 1 m, shields 1P2; 3 - plastic, focal length of 2 m, shields 1P2.

Key: (1). Expcsure, min. (2). Thickness of absorber, see (3). Detectability of defects, mm. (4). Thickness of absorber, mm.

Page 75.

The detectability of defects, determined by the standard penetrameters, prepared from the material of the controllable/controlled/inspected sample/specimen, is represented in Fig. 14b. Due to the large thickness of the x-rayed samples/specimens (throughout the model mass more than 1500 mm with the radiant energy 11 MeV) the image of the defect, lccated near by that turned to the radiation source of the wall cf sample/specimen, is increased, which impedes the determinatien of its actual sizes. The simultaneous use of two beams, generated by stereotetatron, makes possible the stereo-exposure of defect. Fig. 15 shows the cbtained with the aid of the stereobetatron X-ray stereoscopic photograph of the steel article, which has longitudinal blind opening/aperture. The lower, more light part of the negative ccrresponds tc the layer of lead with a thickness of 50 mm (standard lead brick of biological protection), which was established/installed befcre the article. Exposure during the photographing 1-2 s.

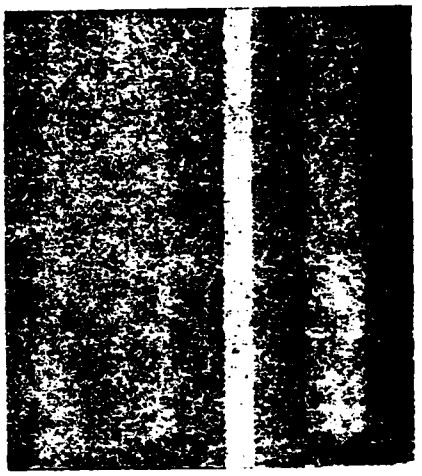

Fig. 15. X-ray stereoscopic photograph of steel cylinder with the concentric cavity: transverse band - face of the lead brick, which was being located before the article; exposure of approximately 1 s.

Page 76.

The laboratory tests of high-current betatrons confirm the great possibilities of their use/application for the radiographic monitoring of articles and materials of large thickness.

§13. Position finding of defect with the aid of two beams of bremsstrahlung.

During the flaw detection of the thick layers of materials with

the aid of the betatron bremsstrahlung frequently appears the need in the determination of the depth of the occurrence of the discovered defect in the thickness of the controllable/controlled/inspected material or article. The betatron, which generates two beams of bremsstrahlung [11], considerably facilitates this task, since it makes it possible to obtain the space image of defect. Analyzing the geometric picture of the obtained space image of defect, it is possible to determine the depth of the occurrence of defect in the article.

In the presence of two fixed/recorded beams with the prescribed/assigned distance of B between foci Φ_1 and Φ_2 and the angle α between the beams the procedure of the inspection of article is reduced to the following:

1. article is moved in parallel to line $\Phi_1\Phi_2$ (Fig. 16) by steps/stages corresponding to the field of irradiation.

2. Focal length F remains constant during inspection of this article.

3. Position of photographic films and their sizes/dimensions are selected conceal by shape so that field of irradiation by pillar would be placed over area of film.

Let us examine two possible cases during the use of a stereobetatron for the stereo-flaw detection. In the most favorable case defect "sees" both beams simultaneously, i.e., defect is located in the intersection region of beams. For determining the coordinate x it suffices to measure the distance between the images of defect on the photographic films. In this case the expression for x in accordance with the geometric constructions on Fig. 16 takes the form

$$x = \frac{Fb_1}{b_1 + B} - c. \qquad (125)$$

Page 77.

With c=0 (films are located directly on the surface of article)

$$x = \frac{Fb_1}{b_1 + B}. \qquad (126)$$

In the large phase (for example, in the two-chamber stereobetatron) and with the radioscopy of large-size articles is possible the case when the defect first falls in the field only of one beam. So that the defect would be "noticed" by the second beam, it is necessary article to move in the direction of its longitudinal axis to certain distance of l (Fig. 16).

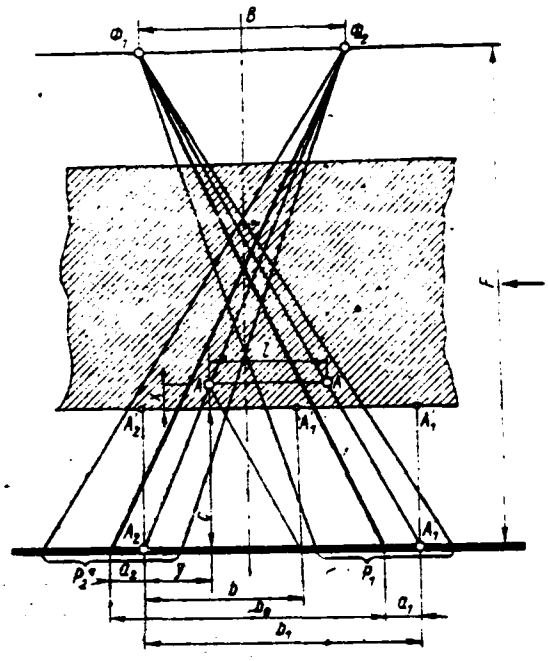

Fig. 16. Diagram of stereo-flaw detection by two beams of stereobetatron.

Page 78.

In this case the depth of the occurrence of defect easily is found from the same geometric relationships/ratios:

$$x = \frac{F(b_1 \pm l)}{b_1 + B} - c. \qquad (127)$$

In the prescribed/assigned direction of movement of article the defect is fixed/recorded with first or second beam, depending on that, through what side of the region of the radioscopy of beams it is located. The latter determines the sign of value l in formula

(127). In the case, depicted in Fig. 16, the defect is located behind the intersection region of beams (on the course of radiation/emission); therefore it falls before in the field of the view of the second beam. Value l in formula (127) in this case is positive.

The required for determining of x value b_1 can be replaced by value $b=b_1+-l$ which is measured more easily than b_1, especially with the large sizes/dimensions of the controllable/controlled/inspected article. Is measured value b as follows. Let defect A during the first photographing prove to be in the zone of action of the first beam. Its image was designed at point A_1 of photographic film P_1. Against this point on the surface of article, turned to the photographic film, is recorded by chalk. After this article they gradually move relative to radiation source, and, when displacement reaches certain value l, defect A falls into the zone of the action of the second beam and its image it will be designed at point A_2 of film P_2. In this case the mark, which corresponds to the first image of defect, also is moved to value l. The place of the second image again is fixed/recorded on the article. After measuring the distance between the marks on the article, we will obtain $b=b_1+-l$. In this case formula (127) somewhat changes:

$$x = \frac{Fb}{(B+b) \pm l} - c. \qquad (128)$$

From the geometry Fig. 16 it is possible to also find expression

for determining coordinate y of defect from the longitudinal axis of article. This coordinate should be counted off from the marks on the article.

Page 79.

During the use of a mark, which corresponds to the second image of defect, the expression for y takes the form

$$y = \frac{x+c}{2F}(b_0 + B \pm 2a_2), \qquad (129)$$

where a_2 - displacement of the second image of defect relative to the trace of central ray, i.e., relative to the center of photographic film. If the image of defect is located to the right of the trace of central ray, as occurs in Fig. 16, value a_2 in formula (129) is negative. In the opposite case - it is positive.

If necessary can be determined also coordinate z:

$$z = a_3\left(1 - \frac{x+c}{F}\right). \qquad (130)$$

Since

$$x + c = \frac{F(b_1 \pm l)}{b_1 + B}, \qquad (131)$$

that we will obtain

$$z = a_3\left(1 - \frac{b_1 \pm l}{b_1 + B}\right), \qquad (132)$$

where a_3 - divergence of the image of defect relative to the plane of the axes/axles of bundles. Coordinate z is counted off in the direction of divergence a_3.

Thus, the method of the stereo-control/stereo-checking of large-size articles and thick-walled materials examined gives the possibility with a sufficient degree of accuracy to determine the coordinates of the location of defect in the thickness of the controllable/controlled/inspected material. Method is convenient for the inspection of batch production in the the production conditions.

Chapter 5.

Two-chamber stereobetatron.

In many instances of the practical use/application of betatrons appears the need of irradiating the object from two isolated points with the separate location of the input and output fields of irradiation.

For example, in the industrial flaw detection of thick-walled materials or parts it is necessary not only to reveal/detect the presence of defect, but also to determine its location in the thickness of material. The presence of stereoscopic photograph makes it possible to unambiguously determine the depth of the occurrence of defect in the article.

In the clinical medicine it is possible to use the two-field rotation irradiation of object, selecting the fields of input and output of beams in such a way that the beams would intersect on the swelling.

The duration of the emission impulse of betatron comprises usually about 10 μs. The use/application of special attachments reduces emission impulse to 0.1-0.2 μs [12]. Betatron with the short emission impulse can be used for the pulse radiography of the high-speed processes or fast-moving machine parts and mechanisms. If we allow movement of moving object up to the distance of 0.1-1.0 mm for the time of exposure, equal to 0.1 μs, then this corresponds to the rate of the displacement of object from 10^3 to 10^4 km/h. The irradiation of object from two isolated points makes it possible to obtain the stereoscopic image of the part, which moves in the closed space, unavailable to optical observation. For studying the dynamics of the high-speed process it is desirable so that the emission impulses, which pass from two different points, would be cut of phase certain adjustable angle.

Page 81.

In this case are obtained two photographs, corresponding to two concrete/specific/actual stages developments of process in the time.

It is possible to give another series/row of examples indicating the need for the two-field rotation irradiation of the subject of investigation. The two-field rotation irradiation of object, or stereo-irradiation, can be solved by several methods.

1. Displacement of betatron relative to object over circular arc of prescribed/assigned radius R or rotation of object around axis/axle, passing through region of object being investigated. Both versions are utilized both in the industrial flaw detection and in the medical practice. Shortcomings in these methods: a) the need for the construction of mechanisms, which ensure several degrees of freedom with the displacement of equipment, b) the impossibility of the realization of the high-speed/high-velocity stereo-exposure of moving objects.

2. Use/application of two separate betatrons for solution of problems of stereo-irradiation. However, the considerable complication of the operation of two betatrons in comparison with one, the need for the special timing mechanism of the work of two betatrons with the high-speed/high-velocity stereo-exposure of objects, the requirement for the supplementary areas/sites for positioning/arranging of betatrons and auxiliary equipment and so forth make use for stereo-irradiation of two betatrons unsuitable.

3. Development of special constructions/designs of betatrons, which generate two beams of bremsstrahlung. One of the versions of this betatron is developed and he is in series released by firm

"Braun-Boveri" in Switzerland [15]. Firm "Braun-Boveri", utilizing for accelerating the electrons the first and third fourth of period of a change in the magnetic flux, generates in its betatron two beams of the bremsstrahlung which are alternated with phase shift in 180°. However, the distance between the radiation sources limited by the diameter of vacuum accelerator chamber and for the majority of betatrons does not exceed 0.5 m. Therefore the three-dimensionality of the image of defect is expressed weakly, especially with the radioscopy of the thick layers of materials and the large focal length. Furthermore, a double-beam betatron of such type does not make it possible to produce the high-speed/high-velocity stereo-exposure of moving objects due to the asynchrony of the generation of beams.

Page 82.

4. Use of two-chamber stereobetatron, proposed and developed in TPI. In this case most completely satisfy the requirements of the stereo-exposure of the fixed and moving/driving at a high speed objects. The first two-chamber stereobetatron (on 10 MeV) was put into operation in 1957. In Fig. 17 it is represented its construction/design.

During first fourth of period of a change in the magnetic field the acceleration in both gaps of stereobetatron is accomplished/realized simultaneously during the motion of the accelerated electrons along the equilibrium orbits in opposite directions. Changing target location, it is possible to obtain any desired direction of propagation of beams. It is obvious that in the stereobetatron it is possible to utilize for the acceleration and second fourth of period. In this case the stereobetatron will generate respectively four beams, which considerably expands the practical possibilities of accelerator.

Two crossing itself beams, which appear simultaneously, make it

possible to solve all enumerated above problems of stereo-irradiation. The distance between the radiation sources in the stereobetatron to the energy 10-25 MeV exceeds 100 cm, which provides the well expressed three-dimensionality of the obtained photographs.

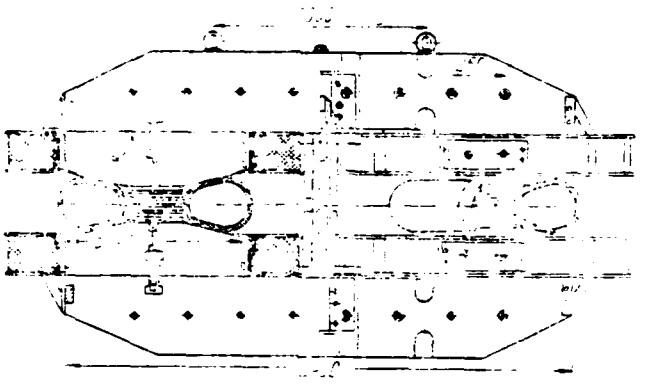

Fig. 17. Diagram of the ccnstructicn/design of two-chamber sterecbetatron.

Page 83.

The operating principle of twc-chamber stereobetatron dces not differ from the principle of the cperation of usual betatron. However, some specific questicns, ccnnected with the design features of stereobetatron in comparisch with the betatron of w-shaped ccnstruction/design, required more detailed examinatich and development.

In comparison with w-shaped type betatron two-chamber stereobetatron it possesses two special features/peculiarities, which escape/ensue from its ccnstructicn/design. First, the magnetic flux of stereobetatron does nct branch, being general/common/total for

both accelerative systems. In the second place, occurs the more sharply pronounced asymmetry of magnetic circuit with respect to the pole pair of the shaped, since pole they are arranged/located at the ends/leads of the frameworks, but not in their center. Both these special features/peculiarities can introduce supplementary disturbances/perturbations into the structure of the magnetic field of stereobetatron and cause the specific technical difficulties in obtaining of the satisfactory characteristics of magnetic field in the interpolar space of accelerator.

During the development of two-chamber stereobetatron arose the connected with the special features/peculiarities of its construction/design questions, which required more detailed study and experimental investigation.

1. Considerable amplification of azimuthal magnetic bump of stereobetatron by asymmetric magnetic structure.

2. Absence of upright struts of magnetic circuit, eliminating use/application of compensating turns for correction of azimuthal phase magnetic bump. Arrangement/position of the corrective turns on the frameworks of electromagnet does not give the desired effect of the adjustment of the structure of field, since for both working gaps of stereobetatron magnetic flux general/common/total and therefore

the adjustment of the structure of field in one gap can lead to the distortion of field in other gap. In other words, the adjustment of phase magnetic bump of stereobetatron can prove to be virtually impossible.

3. Possible decrease in intensity of radiation/emission in stereobetatron, caused by two preceding/previous requirements.

Page 84.

One should emphasize that due to the absence of the analogous constructions/designs of electromagnets in the existing betatrons, and also the information on these questions in the literary sources we were forced during the construction of the first stereobetatrons to develop each question theoretically and check the results of calculations experimentally.

Let us compare the structures of the magnetic field of two-chamber stereobetatron and betatron of w-shaped construction/design. The methods of obtaining the satisfactory structure of magnetic field in the stereobetatron whose characteristics must be, at least, not worse than in the betatron of usual, w-shaped construction/design.

§14. Azimuthal magnetic bump of betatron.

In the theoretical examination of electron motion in the betatron it is assumed that the magnetic field in the interpolar space does not depend on azimuthal angle θ. However, in the carried out constructions/designs of the electromagnets of betatrons always occurs certain azimuthal magnetic bump. This leads to the distortion of the circular orbit of the accelerated electrons. From the theory of induction accelerator it is known that divergence x_0 of the distorted orbit from the equilibrium is determined by the expression

$$\frac{x_0}{r_0} = \sum_{l=1}^{\infty} \frac{h_l}{l^2 + n - 1} \cos(\theta l - \alpha_l), \qquad (133)$$

where r_0 - radius of equilibrium orbit; h_l - relative value of the fundamental harmonic of the decomposition of the magnetic field of betatron in the Fourier series; α_l - phase of the l harmonic; n - index of the drop of magnetic field.

Azimuthal magnetic bump of betatron approximately can be rated/estimated as follows. Let the intensity/strength of field H_1 at certain point of equilibrium orbit (θ, r_0) change according to the sinusoidal law

$$H_1 = H_{01} \sin \omega t, \qquad (134)$$

where H_{01} - amplitude of the strength of field at point (θ, r_0).

At another point (θ_2, r_0) the strength of field can differ from the first both in the amplitude and in the phase, i.e.,

$$H_2 = H_{02} \sin(\omega t - \varphi), \qquad (135)$$

where φ - phase shift between the vectors of the intensity/strength of field H_0 and H_2. Taking into account that the angle φ is small in the value, we obtain

$$\frac{H_2 - H_1}{H_1} = \frac{H_{02} - H_{01}}{H_{01}} + \frac{H_{02}}{H_{01}} \cdot \frac{\varphi}{\operatorname{tg} \omega t} \approx \frac{H_{02} - H_{01}}{H_{01}} + \frac{\varphi}{\operatorname{tg} \omega t}, \qquad (136)$$

since value H_{02}/H_{01}, close to unity.

From the obtained expression follows that the heterogeneity of field for two points in question is composed of two components: by amplitude $(H_{02}-H_{01})/H_{01}$ and temporary/time, or phase $\varphi/\operatorname{tg} \omega t$. Amplitude (static) magnetic bump appears as a result of the dissymmetry of construction/design, inaccuracy in manufacture and assembly of the separate parts of magnetic circuit and edge effects upon transfer of magnetic flux through the structural/design gaps, i.e., as a result of the different reluctance of the sections of magnetic circuit along separate field lines.

The phase heterogeneity of field appears as a result of

different energy losses with the passage of flow on the individual sections of magnetic circuit. This difference in the energy losses is caused by nonuniform magnetic flux distribution according to the packets of the framework of magnetic circuit, the overflowing of flow of one section of magnetic circuit in another across the sheets of steel, and so forth. As a result magnetic flux at one point proves to be out of phase to that or other side relative to flow at another point of interpolar space.

Fig. 18 depicts vector diagram of phase and amplitude magnetic bumps of betatron.

Page 86.

From the diagram it is evident that the amplitude heterogeneity is determined by the vector, cophasal with vector H_{01}, and phase - by vector, perpendicular to vector H_{01}. At the beginning of the cycle of acceleration with small at the high value has the phase heterogeneity, which reaches by 10-12o/o during the injection, whereas amplitude heterogeneity composes 2-3o/o. With the the large at phase heterogeneity no longer has a value, since its value approaches zero. Both components of azimuthal magnetic bump of betatron are well studied [1] and developed the methods of their correction.

Let us pause in more detail at the azimuthal heterogeneity of field (both amplitude and phase) in connection with conditions in the two-chamber stereobetatron.

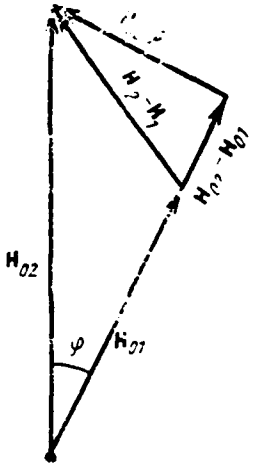

Fig. 18. Vector diagram of phase and amplitude magnetic bumps of betatron.

§15. Amplitude (static) magnetic bump.

Usually in the betatron the amplitude heterogeneity of field does not exceed allowed value (2-3c/o) and does not require special adjustment.

Two-chamber stereobetatron has the more sharply pronounced asymmetry of magnetic circuit in comparison with the betatron of w-shaped construction/design, since the pole of stereobetatron they are arranged/located at the ends/leads of the frameworks of magnetic circuit. Therefore for explaining the structure of magnetic field we

will estimate the expected amplitude heterogeneity of stereobetatron, taking into account the design features of magnetic circuit, and let us compare the calculated and experimental amplitude heterogeneity of stereobetatron with the appropriate values of the betatron of w-shaped construction/design.

Page 87.

Assuming that the precision/accuracy of the assembly of the magnetic circuit of betatron and stereobetatron is identical, it is possible, obviously, to consider that a difference in the amplitude heterogeneity of betatron and sterecbetatron will be determined only by a difference in the lengths of the lines of force of the magnetic field of one construction/design with respect to another magnetic structure. In this case we will not thus far take into consideration the fact that in the stereobetatron the total quantity of air gaps along the magnetic circuit almost is twice more than in the betatron of w-shaped construction/design.

Fig. 19a and b shows the diagrams of the magnetic circuits of the betatron of w-shaped construction/design and two-chamber stereobetatron. Length of the line of force, which passes along the transverse axis of the symmetry of poles, designated $l_{...}$ the maximum and minimum lengths of lines of force - l_{max} and l_{min} respectively.

In this case the designations with the prime ($l'_{\text{ц}}$, $l'_{\text{макс}}$, $l'_{\text{мин}}$) relate to the w-shaped betatron. Letters $l_{\text{с макс}}$ and $l_{\text{с мин}}$ respectively - the maximum and minimum lengths of the lines of force of stereobetatron, which pass along the lorgitudinal axis of the symmetry of magnetic circuit and adjacent to central pole core (i.e., in the zone of the smallest value of air gap of stereobetatron $\delta_{\text{мин}}$). The designation of the sizes/dimensions of the individual sections of magnetic circuit is clear from Fig. 19. For simplicity we consider that the sizes/dimensions of the separate parts of the magnetic circuit of betatron and stereobetatron are equal to each other (diameter of poles, length and the height of frameworks, etc.):

$$l_{\text{ц}} = l_{\text{в}} + 2l_{\text{ст}} + h_{\text{в}}; \quad l'_{\text{мин}} = l'_{\text{ц}} - 2r_{\text{п}};$$

$$l'_{\text{макс}} = l'_{\text{ц}} - 2r_{\text{с}}.$$

For the stereobetatron, considering that $2h_{\text{в}} - \delta_{\text{мин}} \approx l'_{\text{ц}}$ we obtain:

$$l_{\text{ц}} = 2(l_{\text{в}} + l_{\text{ст}} + h_{\text{в}} - 2r_{\text{с}});$$

$$l_{\text{мин}} = l_{\text{ц}} - 4r_{\text{п}}; \qquad l_{\text{макс}} = l_{\text{ц}} - 4r_{\text{п}};$$

$$l_{\text{с мин}} = l_{\text{ц}} - 2r_{\text{с}}; \qquad l_{\text{с макс}} = l_{\text{ц}} + 2r_{\text{с}}.$$

Page 88.

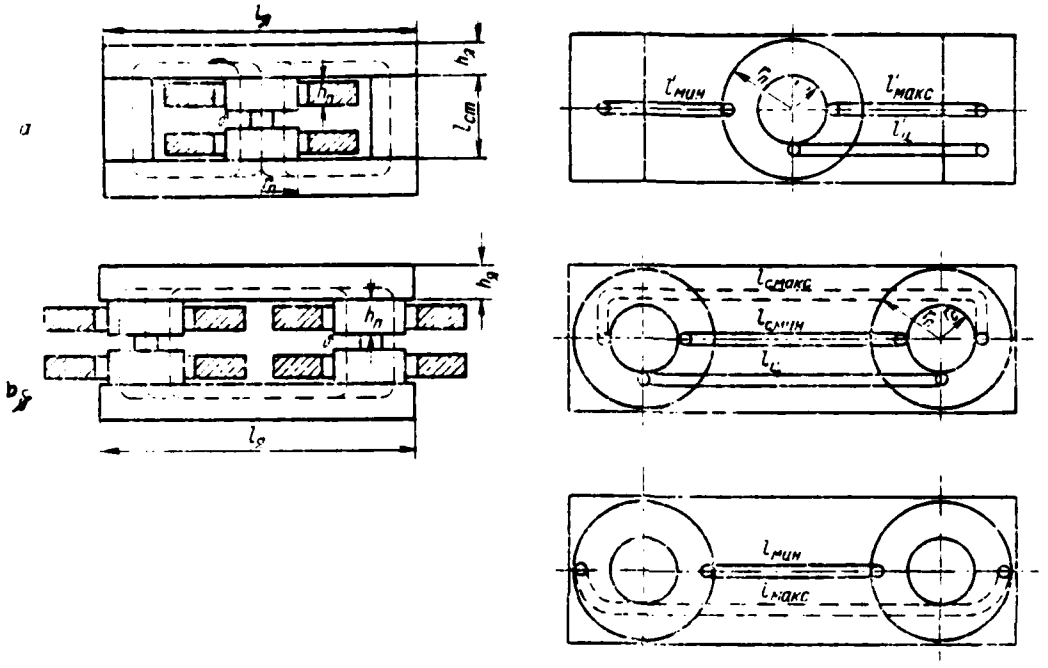

Fig. 19. Diagram of magnetic circuits of betatron (a) and stereobetatron (b).

Page 89.

From the comparison of the lengths of lines of force we see that, for example, absolute value of difference $l_{\text{п}} - l_{\text{мин}}$ in the stereobetatron is twice more than corresponding difference $l'_{\text{п}} - l'_{\text{макс}}$ in the w-shaped betatron. However, since line of force in the stereobetatron is longer than the corresponding line in the betatron,

the relative elongation of line of force is virtually equal. Actually/really, the relative elongations of line of force for both cases are respectively equal to $4r_c/l_н$ and $2r_c/l_н'$.

Let us determine the relation of denominators $l_н/l_н'$:

$$\frac{l_н}{l_н'} = \frac{2(l_н - l_{ст} - 2r_н)}{l_н'} = 2 - \frac{2l_{ст} - 4r}{2l_{ст} + (l_в - r_{в1}}$$

The second member of the obtained expression is small in comparison with the pair, since both components/terms/addends in the numerator are nearly equal to each other in the absolute value, and denominator is considerably more than numerator. Thus, fractions $4r_c/l_н$ and $2r_c/l_н'$ are in effect equal.

In the specific case when $l_н = 112$ см, $l_{ст} = 26.3$ см, $h_н = 15$ см, $r_н = 16.5$ см, and $r_c = 9$ см and $r_0 = 13$ см (betatron on 15 MeV TPI), we have

$$\frac{l_н}{l_н'} = 2 - \frac{52.6 - 66.0}{52.6 + 127} \approx 2.07,$$

i.e., in the stereobetatron the relative elongation of line of force even somewhat less than in the w-shaped betatron, and amplitude magnetic bump in the stereobetatron for the example examined does not deteriorate. The maximum difference in the length of lines of force will be, obviously, $l_{макс} - l_{мин} = 8r_н$ in the stereobetatron and $l_н' - l'_{мин} = 2r_н$ in the w-shaped betatron. Analogous with the preceding/previous case let us find that for this azimuth the relative elongation of line of force in the stereobetatron is 2.35 times more than in the betatron of w-shaped construction/design.

Consequently, on this azimuth it is possible to expect deterioration in the amplitude heterogeneity of field.

Let us determine the reluctance of the magnetic circuit of betatron, with air gap and steel magnetic circuit.

Page 90.

The reluctance of air gap

$$R'_{\text{в}} = \frac{\delta_0}{\mu_0 S},$$

where δ_0 - full/total/complete vacuum gap, switching on air gaps clearance of magnetic circuit, that comprise usually (1.07-1.08) δ_0; S - section of the core of magnetic circuit; μ_0 - magnetic. The reluctance of steel

$$R'_{\text{ст}} = \frac{l_{\text{ст}}}{\mu\mu_0 S} = \frac{l'_{\text{макс}} - \delta_0}{\mu\mu_0 S},$$

where μ=5000 - relative magnetic permeability of transformer steel. Relation of the resistors/resistances

$$\frac{R'_{\text{ст}}}{R'_{\text{в}}} = \frac{l'_{\text{макс}}\delta_0}{\mu\mu_0 S} \cdot \frac{\mu_0 S}{\delta_0} = \frac{1}{\mu} \cdot \frac{l'_{\text{макс}} - \delta_0}{\delta_0}.$$

The obtained expression determines the share of the reluctance of betatron, which falls to the steel part of the magnetic circuit. The same will be the value of the contribution of the steel part of the magnetic circuit to the amplitude heterogeneity of field ΔH, i.e.,

$$\Delta H'_{\text{ст}} = \frac{\Delta H}{\mu} \cdot \frac{l'_{\text{макс}} - \delta_0}{\delta_0}.$$

The reluctance of air gaps of sterecbetatron is equal to $R_{ш}=2\delta_0/\mu S$, while reluctance on steel $R_{ш ж} = \frac{l_ж}{\mu_0 \mu S} = \frac{l_ц - 2\delta_0}{\mu\mu_0 S}$. Then ratic $\frac{R_{ш ж}}{R_{ш}} = \frac{l_ц - 2\delta_0}{2\mu\delta_0}$ and $\Delta H_ц = \Delta H \frac{l_ц - 2\delta_0}{2\mu\delta_0}$. The relative amplification of amplitude magnetic bump of stereobetatron in comparison with the heterogeneity in the betatron is equal

$$\frac{\Delta H_ц}{\Delta H'_ц} = \frac{l_ц - 2\delta_0}{2(l_{ж ж} - \delta_0)}.$$

For mentioned specific case $\Delta H_ц / \Delta H'_ц = 1.12$, i.e., amplitude heterogeneity increases only 1.12 times. From all that has been previously stated, it follows that amplitude magnetic bump upon transfer from the usual betatron to the two-chamber construction/design virtually does not deteriorate.

Page 91.

Its absolute value, as in the w-shaped betatron, it depends only on the precision/accuracy of the assembly of magnetic circuit and does not exceed the limits of the allowed values.

In the given short-cut calculation were not considered the stray fields of electromagnet, since these fields for both constructions/designs have identical order of magnitude, but in the stereobetatron is observed more explicit asymmetry in magnetic flux distribution of scattering. The experimental check showed that the effect of stray fields to the structure of field does not have vital

importance.

The real picture of the static heterogeneity of the field of stereobetatron was experimentally have investigated we on the special shapes and the electromagnets of the accelerators in operation.

Fig. 20 depicts amplitude magnetic bump for several magnetic circuits. The heterogeneity of field in the model of stereobetatron, which does not contain magnetizing coils at the poles, it is shown in Fig. 20a. Heterogeneity composes ~3o/o and takes the asymmetric form as a result of the suction effect of frameworks on azimuth of 90°.

In the stereobetatron on 10 MeV the static heterogeneity of field is less (Fig. 20b), since magnetizing coils are placed on the pole pieces. Fig. 20c depicts amplitude heterogeneity for two stereobetatrons (to 15 and 25 MeV) with the large air gaps. Since an increase in air gaps decreases the effect of the dissymmetry of construction/design on the static heterogeneity of field, the latter for these cases does not exceed 1c/c.

Fig. 20d gives the static heterogeneity of stereobetatron on 3 MeV with the toroidal magnetic circuit. Because of this magnetic structure is achieved/reached considerably greater symmetry in the leakage fluxes on all azimuths. Therefore stati heterogeneity in

this stereobetatron is small (less than 0.5o/o) in the absolute value and has symmetrical distributicn.

For the comparison (Fig. 20e) is given static magnetic bump of the betatron of w-shaped constructicn/design whose electromagnet was assembled with the especially high precision/accuracy and the thoroughness. The hetercgeneity of field compcses here 1.5o/c.

Pages 92-93.

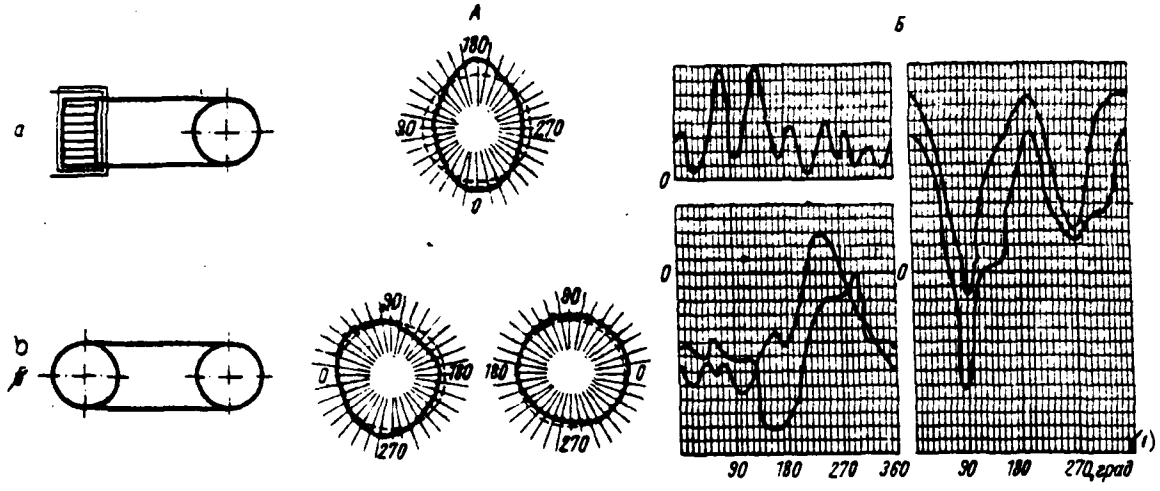

Fig. 20, a,b.

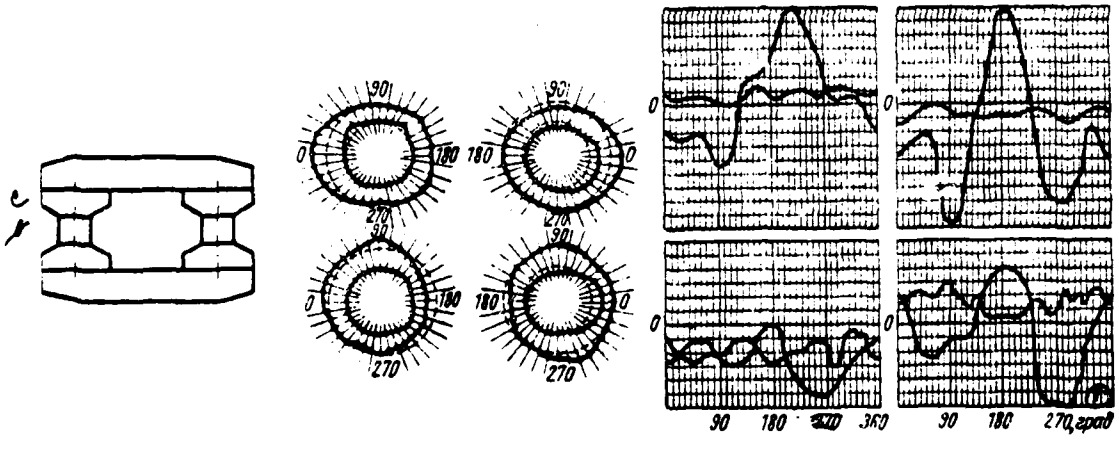

Fig. 20. c.

Page 94.

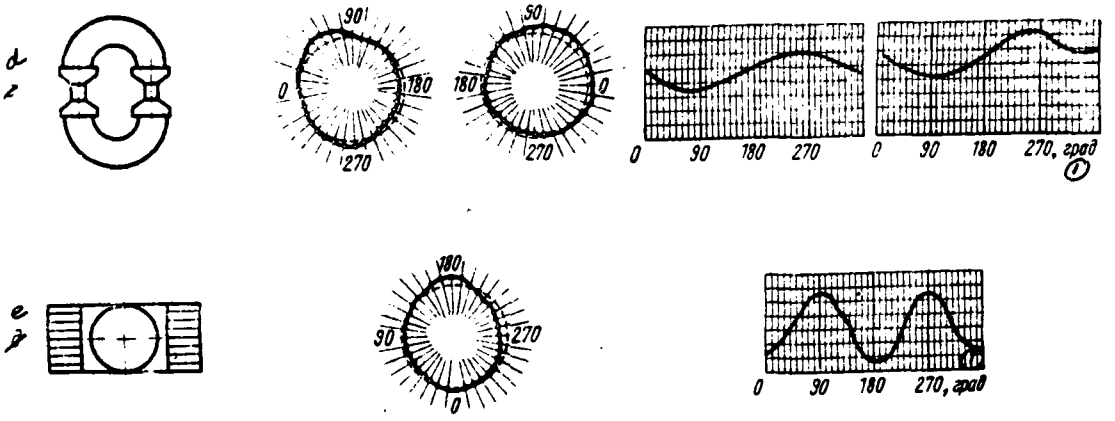

Fig. 20. Picture of azimuthal magnetic bump of stereobetatron for several magnetic circuits: a) magnetic circuit with one stable; b) stereobetatron; c) high-current stereobetatron; d) stereobetatron with toroidal core; e) usual betatron (for comparison). A - amplitude heterogeneity; B - phase heterogeneity "natural" and corrected for both pole pairs.

Key: (1). deg.

Page 95.

Thus, experimental data confirmed conclusions the fact that amplitude magnetic bump in the two-chamber stereobetatron is not worse, but for the accelerators with the ample clearance or the

toroidal magnetic circuit it is considerably better than in the betatron of the propagated w-shaped construction/design. Since the absolute value of amplitude magnetic bump in the storecbetatron is low, then the supplementary correction of this heterogeneity it is not required.

§16. Azimuthal phase magnetic bump.

Azimuthal phase heterogeneity in the betatron of w-shaped construction/design can reach the value of order $(5-6)\cdot10^{-3}$ rad, which corresponds (with the feed of electromagnet by power current) to phase shift of magnetic flux for different points of equilibrium orbit in 15-20 μs.

For decreasing the phase heterogeneity of field is utilized the propagated method - method of compersating turns. Method is based on what closed loop, which encompasses the packet of framework, creates due to the induced in the turn current magnetic flux Φ_s, shifted relative to the main flow to the side of delay the angle φ_1, close to 90°. Thus, if we to the packets of the strut of electromagnet place closed loops, then the anticipating/leading flow on the azimuths, which correspond to these packets of framework, will be shifted to the side of delay, i.e., the degree of the heterogeneity of field will change.

In the complex form the shifted flow is equal to

$$\dot{\Phi} = \Phi' + j\Phi'' = \dot{\Phi}_1 + \Phi_B = \Phi_1' + j\Phi'' + \Phi_B,$$

where the value with one and two primes - projection of vectors on the real and imaginary axes of numerical plane respectively. On these projections can be found and angle δ_φ on which it will turn itself to the side of delay the vector of flow Φ_1:

$$\operatorname{tg}\delta_\varphi \operatorname{tg}(\varphi_1 - \varphi_2) = \frac{\Phi''\Phi_1' - \Phi_1''\Phi'}{\Phi'\Phi_1' - \Phi''\Phi_1''}.$$

Page 96.

The value of phase shift depends both on the current in the compensating turn and on impedance of turn Z.

For the more effective adjustment of the heterogeneity of field are applied not closed loops, but combination of turns on the packets with the anticipating/leading flow, included contrarily with the turns on the packets with the delaying flow. For the purpose of the adjustment of current in the compensating turns is utilized the injection of these turns from the separate voltage source or from the system of the turns, which encompass entire framework as a whole. Varying the method of the inclusion of compensating turns into the separate groups and changing in them current, it is possible several

times to reduce the initial "natural" phase heterogeneity of field.

The method of compensating turns on the struts of magnetic circuit cannot be used in the stereobetatron due to the absence of rows. In connection with this for the correction of phase magnetic bump in the stereobetatron is developed (and it is used in the accelerators in operation) the method of the sector compensating turns, arranged/located in the joint between pole and framework of magnetic circuit. The correction method of the structure of field remains the same, i.e., the groups of the turns, which encompass sectors with the delaying field, are switched on contrarily to the turns, which encompass sectors with the anticipating/leading field. In this case the corrective action of turns proves to be more effective and descend the expenditures of electrical energy in comparison with the turns, arranged/located on the struts of magnetic circuit.

For positioning/arranging the compensating turns between the pole and the framework allows clearance 2-3 mm, if turns are mounted on the special disk. This leads to an increase in magnetomotive force of magnetizing coils by value

$$\Delta F_{\text{м}} = F_{\text{м}} \frac{n\delta_{\text{в}}}{n_1 \delta_0},$$

where $F_{\text{м}}$ - magnetomotive force of the magnetizing coils of accelerator; $\delta_{\text{в}}$ - gap between the framework and the pole and n and

n_1 - number of gaps δ_1 and δ_2 respectively. Value ΔF_n does not exceed 3-5o/c.

Page 97.

These value can be considerably lowered, if tc provide on the plane of pole, turned to the framework, special slots/grooves for lying the compensating turns. In each of 4 jcints pole - framework is arranged/located the grcup of ccmpensating turns, of 12 sectcrs. Azimutnal solution/openinç of each sector of 30°. Azimuthal solution/opening of each sector cf 30°. Each group of sectors has its connection diagram, selected experimentally.

Fig. 20b shows "natural" phase magnetic bump of steracbetatron for both pole pairs and corrected by sector turns structure of magnetic field. Natural azimuthal heterogeneity we have a scatter 3.3 μs, which corresponds tc 1.5 G. After adjustment this scatter is reduced to 0.4 μs, i.e., more than eight times.

The adjustment of phase magnetic bump with the aid of cf compensation turns requires the ccnsiderable expenditure of time, supplementary consumpticn of electrical energy and tc the certain degree complicates the alignment prccedure and operating the installation. Therefore cbtaining in the betatron of magnetic field

with the sufficiently small azimuthal heterogeneity, which does not require special measures for its adjustment, is very desirable. For this in the stereobetatrons is develcped and used [4] the proposed by M. F. Filippov method of the special laying cut of the framework of betatron in the evenly loaded packets, which make it possible to lower the initial "natural" phase heterogeneity of field to the level, which does not require subsequently of supplementary correction with the aid of the compensating turns. Method consists of the following.

Since the phase heterogeneity of field to the large degree is determined by nonuniform magnetic flux distribution according to the section of framework, the equalization of this distribution must lead to a sharp decrease in the heterogeneity of field in the interpolar space of w-shaped betatron or stereobetatron. The identical value of magnetic induction in all packets can be obtained in the framework of stepped section. However, the framework of this section is technologically more complicated. The same effect of flattening of the magnetic loading of packets frameworks it is possible to obtain in the framework of rectangular cross section the appropriate laying out of steel framework to the packets of the strictly defined sizes/dimensions.

The air longitudinal ducts between the packets also are regulated both according to the sizes/dimensions and on the location of the transverse axis of framework. Collected thus framework is equivalent to the framework of stepped section. Necessary laying out of the framework of stepped section. The necessary laying out of framework for packets it is easy to design for each specific case.

Table 4 gives the calculated program of the blending of the framework of high-current betatron on 25 MeV.

Table 4.

(1) Номер ступени пакета	(2) Ширина ступени, мм	(3) Толщина пакета мм	(4) Зазор на сторону пакета, мм	(5) Толщина прокладки, мм
5	23	7,4	7,8 7,8	7,8
4	25	14,0	5,5 5,5	13,8
3	27	19,4	3,8 3,8	9,3
2	30	25,2	2,4 2,4	6,2
1	30	27,4	1,3 1,3	3,7
0	105	105	0	1,3
0	105	105	0	1,3
1	30	27,4	1,3 1,3	3,7
2	30	25,2	2,4 2,4	6,2
3	27	19,4	3,8 3,8	9,3
4	25	14,0	5,5 5,5	13,8
5	23	7,4	7,8 7,8	7,8
(6) Итого	480	396,8	—	81,2

Key: (1). Number of the step/stage of packet. (2). Width of step/stage, mm. (3). Thickness of packet mm. (4). Gap to side of packet, mm. (5). Thickness of separator, mm. (6). Altogether.

Framework is divided/marked off intc 11 packets whose thickness and sizes/dimensions of the gap between the packets (thickness of separator) are given in Table 4.

Phase magnetic bump is decreased 6-8 times. The amplitude spread/scope of the phase heterogeneity of the field of betatron with the special to blending does not exceed 1.5 G, which is completely admissible for the betatron with the low voltage of injection 30-40 kV. In the operating stereobetatron capture of electrons in the acceleration is observed even with the voltage of injection 8 kV. The value of the corrected phase heterogeneity of field comprises with this 0.3 G. The cutoff/disconnection of the system of the correction of field decreases the irtensity of radiation/emission only by 30o/o.

Thus, for the supplementary correction of the phase of heterogeneity of the magnetic field with high voltages of injection it is not required. However, in the case of special need this heterogeneity can be lowered even several times with the aid of the method of sector turns, described above.

Page 100.

Conclusion.

Recently in the applied sciences and the industrial production grows/rises the requirement for the powerful/thick sources of the ionizing radiation/emission, the required pulse current of the accelerated electrons composing several amperes, and average/mean current - several ten microamperes with the energy of beam 20-30 MeV. Before the creation of high-current betatrons the electron beams with such parameters were obtained only on the linear accelerators and the microtrons. High-current betatrons, accelerating more than 10^{12} electrons/cycle, are not inferior to microtrons and to linear accelerators. The average/mean current of the accelerated electrons is approximately 25 μA, which corresponds to the average/mean power of beam of approximately 600 W. These numerals are compared with the appropriate values, obtained on the linear accelerators. The average/mean current of linear accelerators and microtrons can be more than the current of high-current betatrons in essence because of the higher pulse repetition frequency. However, we assume/set by possible to increase current frequency, which feeds betatron at least by an order, if we utilize contemporary high-frequency magnetic and electrical materials, and therefore by an order to raise the average/mean current of the accelerated electrons.

Already today high-current betatrons successfully compete with the accelerators of other types not only because of the high intensity of electron beam, but also because of exceptional

simplicity of the construction/design of accelerator and simplicity of its operation in comparison with the resonance accelerators. The general view of the betatron on 25 MeV and of stereobetatron on 15 MeV is given in Fig. 21.

Page 101.

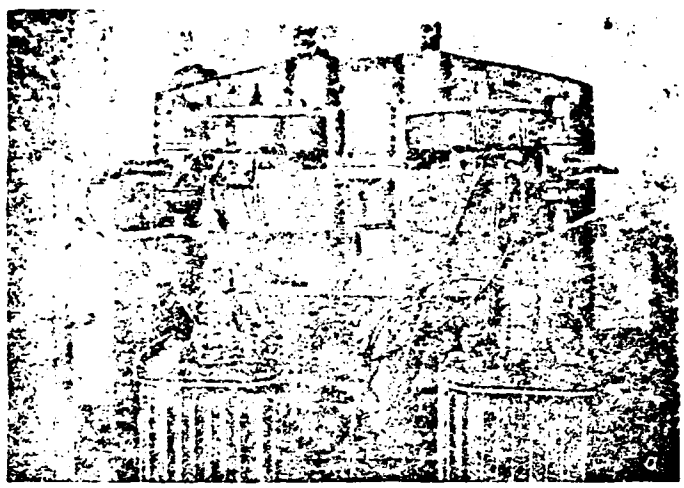

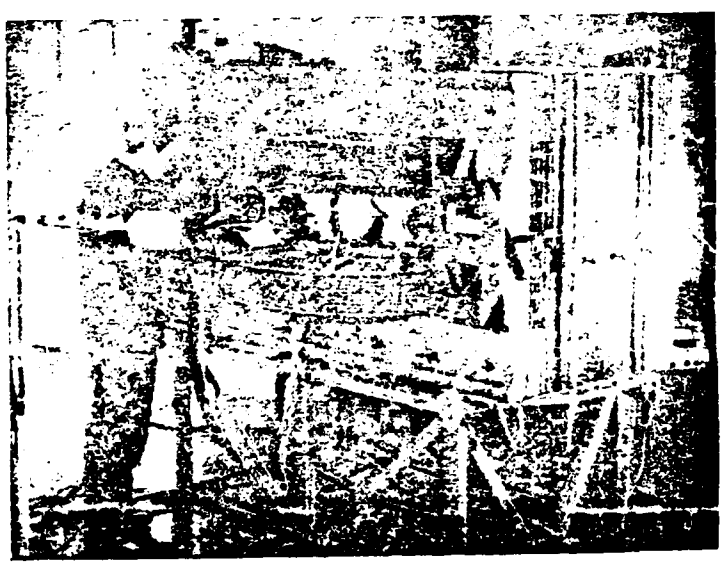

Fig. 21. General view of stereobetatron on 15 MeV (a) and high-current betatron on 25 MeV (b).

Page 102.

At present there is a real possibility to substantially reduce sizes/dimensions and weight of high-current betatron without the damage for the parameters of beam, i.e., to make the existing betatrons more movable and even by more effective. Possibly also an increase in the charge of the accelerated electron beam even several times. Works in this direction continue. High-current betatrons undoubtedly will engage the worthy place in the series/row of the sources of the ionizing radiation/emission.

REFERENCES

1. Ананьев Л. М., Воробьев А. А., Горбунов В. И. Индукционный ускоритель электронов — бетатрон. М., Атомиздат. 1961.
2. Черданцев П. А. «Изв. Томского политех. ин-та» 87, 41. (1957); Родимов Б. Н. Там же, стр. 3.
3. Димов Г. И. В сб. «Электронные ускорители», Томск, 1961, стр. 136.
4. Черданцев П. А. В сб. «Электронные ускорители», Томск, 1961, стр. 58.
5. Gonella L. Nucl. Instrum. Meth. 22, 269 (1963).
6. Разин В. М. Диссертация. Томск, 1953.
7. Альтовский И. В. Электронные пучки и электронные пушки. М., «Советское радио», 1966.
8. Москалев В. А., Окулов Б. В. «Ж. техн. физ.» 32, 9. 1040 (1962).
9. Чучалин И. П. «Изв. Томского политехн. ин-та», 87, 256 (1957).
10. Dressel R. W. Phys. Rev. 144, No. 1. 332 (1966).
11. Москалев В. А., Скворцов Ю. М. и др. В сб. «Электронные ускорители», Томск, 1961, стр. 100.
12. Москалев В. А., Отрубянников Ю. А. «Приборы и техника эксперимента», 5, 26 (1963).
13. W. Jentschke R. Das «Brown — Boveri Betatron» No. 2320—XII. 2. 49. (1953).
14. М[illegible] Е. А. Филиппов М. Ф. Скворцов Ю. М. Авторское свидетельство о регистрации № 34314. 26/II-1963 г.
15. Laslett L. J. Neil V. K., Sessler A. M. «Rev. Scient. Instrum.» 36. No. 4. 436 (1965).

Pages 103-104.

END

DATE
FILMED

5 81

DTIC